PERGAMON

Journal of the Mechanics and Physics of Solids
47 (1999) 1663–1697

JOURNAL OF THE
MECHANICS AND
PHYSICS OF SOLIDS

A constitutive model for ferroelectric polycrystals

J.E. Huber[a], N.A. Fleck[a,*], C.M. Landis[b], R.M. McMeeking[b]

[a] *Cambridge University Engineering Department, Trumpington Street, Cambridge, CB2 1PZ, U.K.*
[b] *Department of Mechanical and Environmental Engineering, University of California, Santa Barbara, California 93106, U.S.A.*

Received 1 September 1998; received in revised form 29 November 1998

Abstract

A constitutive model is developed for the non-linear switching of ferroelectric polycrystals under a combination of mechanical stress and electric field. It is envisaged that the polycrystal consists of a set of bonded crystals and that each crystal comprises a set of distinct crystal variants. Within each crystal the switching event, which converts one crystal variant into another, gives rise to a progressive change in remanent strain and polarisation and to a change in the average linear electromechanical properties. It is further assumed that switching is resisted by the dissipative motion of domain walls. The constitutive model for the progressive switching of each crystal draws upon elastic–plastic crystal plasticity theory, and a prescription is given for the tangent moduli of the crystal, for any assumed set of potentially active transformation systems. A self-consistent analysis is used to estimate the macroscopic response of tetragonal crystals (representative of lead titanate) under a variety of loading paths. Also, the evolution of the 'switching surface' in stress-electric field space is calculated. Many of the qualitative features of ferroelectric switching, such as butterfly hysteresis loops, are predicted by the analysis.

Keywords: A. Twinning; B. Crystal plasticity; Ferroelectric switching

1. Introduction

Ferroelectrics are piezoelectric materials with the ability to switch their polarisation direction under an applied electric or mechanical field (Jaffe et al., 1971; Lines and

* Corresponding author. Tel.: 01223 332650/332600; fax: 0044 01223 332662; e-mail: naf1@eng.cam.ac.uk

0022-5096/99/$ - see front matter
PII: S0022-5096(98)00122-7

Glass, 1977). A robust constitutive model that captures ferroelectric switching is desirable in order to guide the processing and development of ferroelectrics and for use in the design of ferroelectric devices. The aim of this paper is to develop a non-linear constitutive law for the switching of ferroelectrics, using an approach similar to that of crystal plasticity theory.

Polycrystalline ferroelectric ceramics are commonly used for acoustic sensors, such as hydrophones (Newnham et al., 1990). Other uses include actuators for vibration and noise suppression, for aerofoil control surfaces and for the end effectors of robots (Ghandi and Thompson, 1992). Some of these devices have complicated configurations, such as multilayer stacks or interdigitated electrodes. The initial pattern of polarisation in these components is impossible to predict from simple analysis. High stress and high field areas exist within the ceramic at geometric discontinuities such as corners and the tips of electrodes. Such regions are troublesome as they can lead to delaminations of the electrodes and to fatigue cracking and failure of the device (Winzer et al., 1990; Pepin and Boyland, 1989). Furthermore, stresses generated during operation can cause depolarisation and therefore make the material ineffective for actuation. This makes it difficult to design such a device to achieve the required actuation motions and forces except by trial and error. These considerations indicate that a non-linear constitutive law is needed for the improved design of ferroelectric devices. With such a constitutive law, calculations could be carried out to predict the polarisation and piezoelectric responses of practical devices.

The most widely used ferroelectrics are barium titanate, lead zirconate titanate (PZT) and lead lanthanum zirconate titanate (PLZT), which have perovskite-type structures. In the paraelectric (i.e. non-ferroelectric) state, the unit cell for these perovskites is cubic. A typical example for lead titanate is shown in Fig. 1(a). Below a critical temperature T_c, called the Curie temperature, the unit cell is non-cubic and the material is piezoelectric and ferroelectric. The example shown in Fig. 1(a) involves a tetragonal unit cell below the Curie temperature. Although other crystallographic

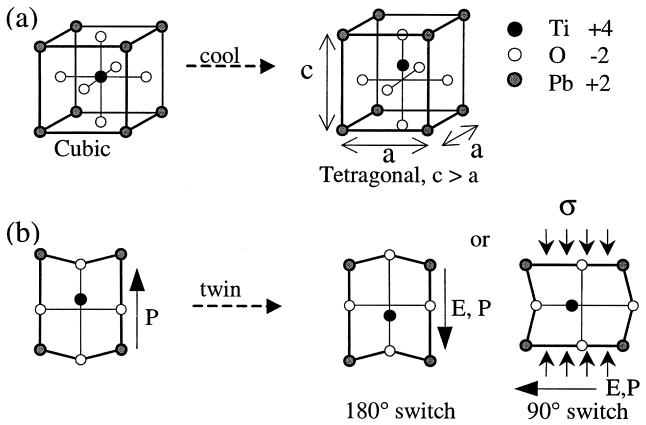

Fig. 1. (a) Transformation from the cubic to the tetragonal unit cell of lead titanate at the Curie temperature; (b) twinning of tetragonal lead titanate under stress or electric field.

structures, such as rhombohedral, do arise (Lines and Glass, 1977) we will focus on materials which are tetragonal in the ferroelectric state. In the tetragonal unit cell, a dipole moment of the charge distribution exists, such that the mean centres of ions of opposite charge do not coincide. Thus, the unit cell possesses a spontaneous polarisation and a spontaneous strain aligned with the dipole moment, see Fig. 1(a).

The crystal lattice of such a material is piezoelectric. When a tensile stress is applied parallel to the polarisation direction, the charge centres separate further, leading to a change in the polarisation which is linear (to leading order) in the applied stress. The polarisation change can be measured as follows: a change in the polarisation produces surface layers of bound charge which attract or repel free charge in an external electrical circuit. When an electric field is applied parallel to the spontaneous polarisation the effective charge centres move and a strain is induced in the crystal; this effect is also linear to leading-order. Lead based perovskites are particularly attractive piezoelectrics for both sensor and actuator applications as they possess high cross-coupling between mechanical and electrical fields (Jaffe et al., 1971; Lines and Glass, 1977).

If a sufficiently large electric field is applied to a ferroelectric, the direction of spontaneous polarisation can change by 90 or 180°, as illustrated in Fig. 1(b). The 180° switch is accommodated with unchanged tetragonality of the unit cell, whereas the 90° switch is accompanied by a reorientation of the tetragonality. Note that the 90° switch can also be induced by applied stress $\boldsymbol{\sigma}$. Since there are six equivalent crystallographic directions in the tetragonal structure, there are always four possible 90° switches and one 180° switch. (For other crystallographic structures such as rhombohedral, there exist other switches conforming to the isomorphisms of the unit cell.) Ferroelectricity is defined by the ability of a crystal to switch its polarisation in response to an applied electrical or mechanical field.

Polycrystalline ferroelectrics of the perovskite oxide family are usually prepared by a mixed-oxide processing route (Jaffe et al., 1971; Lines and Glass, 1977). After sintering the material is paraelectric until the temperature is reduced to below the Curie level, at which point the individual crystals progressively transform to a tetragonal state (Lines and Glass, 1977). Since the crystallographic axes are random from grain to grain within the polycrystal, there are mismatches of spontaneous strain and polarisation from grain to grain. In order to minimise the free energy associated with this mismatch, domains, which are regions of differing polarisation, are induced within the crystals. Adjacent domains are separated by domain walls, across which the spontaneous polarisation is discontinuous. As a result of the domain structure, the average polarisation and tetragonality of each crystal within the ceramic is low; when the polarisation and tetragonality are further averaged over all crystals, they are essentially zero. Local piezoelectric action is present within the individual crystals, but the effect averaged over the entire polycrystal is zero. Thus, prior to poling, the polycrystal is macroscopically isotropic and has no piezoelectric properties.

The material is poled by the application of a large electric field. This has the effect of switching many of the domains to a polarisation direction more closely aligned with the applied electric field. The structure within each crystal is reorganised, such that many crystals are composed of a single or a few favourably polarised domains.

After poling, the polycrystal has an average polarisation and strain and is macroscopically piezoelectric.

Recently, several approaches have been used to model the non-linear behaviour of ferroelectrics (Chan and Hagood, 1994; Hwang et al., 1995, 1998) and of transforming solids in general (Ball and James, 1987, 1992). The strategy developed by Ball and James is mathematically rigorous, seeking local energy minima and has been applied in the study of shape memory polycrystals (Bruno et al., 1996; Smyshlyaev and Willis, 1998). This type of approach neglects the dissipation of energy associated with domain wall motion and does not capture hysteresis of the type found in ferroelectrics. In order to develop a model which incorporates dissipation, it is necessary to consider the resistance to domain wall motion arising from anharmonic lattice interactions and from pinning defects such as dopant ions and ion holes (Jaffe et al., 1971).

A constitutive law for domain wall motion can be constructed by balancing the free energy reduction with the energy dissipated when domain walls move (Abeyaratne and Knowles, 1990; Jiang, 1993, 1994; Loge and Suo, 1996). Models of this type have been combined with homogenisation techniques to predict the macroscopic behaviour of polycrystalline ferroelectric ceramics (Chan and Hagood, 1994; Hwang et al., 1995, 1998; Hwang and McMeeking, 1998a, b, c). In these treatments, domains are identified by their crystallographic orientation and are assumed to switch completely between distinct states of strain and polarisation when a free energy reduction criterion is met. The sophistication of these models ranges from Taylor-like in which interactions among the crystallites are neglected (Hwang et al., 1995) to treatments by the finite element method in which crystallite interactions are fully accounted for (Hwang and McMeeking, 1998b, c). In between are schemes which assume Gaussian fluctuations imposed on a Taylor model (Chan and Hagood, 1994) and schemes which account for interactions by a mean field theory (Hwang et al., 1998; Hwang and McMeeking, 1998a). These models are able to reproduce several aspects of the behaviour of ferroelectric polycrystals. In particular, dielectric hysteresis in the electric displacement versus electric field response and 'butterfly' hysteresis in the strain versus electric field curve can be captured.

Some improvements to the previous models are desirable on physical grounds and have the potential to improve the accuracy of predictions of the material behaviour. In particular, the assumption that domains switch completely between distinct states of strain and polarisation is inaccurate. It is observed experimentally that a single crystal switches by the progressive movement of domain walls, driven by a combination of electric field and stress. A constitutive model, which incorporates progressive transformation by domain wall motion, is presented in this paper. The model is based on the observation that an incremental transformation by domain wall motion is equivalent to incremental slip on a crystal slip system (Huber, 1998). This allows for the adaptation of established models of crystal plasticity for use with ferroelectric switching: crystal plasticity theory as developed by Hill (1966) and employed by Hutchinson (1970) is readily modified to the coupled ferroelectric case. The constitutive model developed here is general, allowing for any crystal structure and taking account of features such as the change of piezoelectric properties during transformation and the saturation of switching upon complete transformation. The

model contains as special cases earlier models employed in the study of crystal plasticity (Budiansky and Wu, 1962; Hutchinson, 1970). In the mechanical limit, the switching process is known as twinning and is the basis of transformation plasticity in metals such as shape memory allows. Several related models for twinning in shape memory alloys exist (Patoor et al., 1994; Lagoudas and Bhattacharyya, 1997; Huang and Brinson, 1998). These models typically use the volume fractions of each crystal variant as kinematic variables, but differ in the way they relate the macroscopic values of stress and strain to the local values. Lagoudas and Bhattacharyya discuss several schemes for relating the macroscopic and local values of stress and strain. These include Mori–Tanaka averaging and the self-consistent method. Huang and Brinson use the Eshelby–Kröner approach to account for the interaction energy between distinct variants in a single crystal formulation; they allow for the concurrent growth of groups of variants which produce zero overall transformation strain. A useful summary of recent models for twinning in shape memory alloys is given by Huang and Brinson (1998).

As an application of the constitutive model for ferroelectrics developed here, a self-consistent mean field homogenisation scheme for a ferroelectric polycrystal is developed, along the lines of the self-consistent mechanics proposed by Hill (1965a, b). This scheme is used to predict the non-linear switching response of a ferroelectric polycrystal to electrical and mechanical loading, including the evolution of switching surfaces in stress and electric field space.

2. Governing field equations

In a ferroelectric, domain wall motion within each crystal leads to a change in the remanent strain and polarisation. This non-linear switching closely resembles plastic deformation by slip in a metallic polycrystal: domain wall motion is treated in the same manner as slip in elastic–plastic crystals.

Consider an anisotropic ferroelectric solid subjected to an electric field E_i and to a mechanical stress σ_{ij}. On introducing the notation superscript 'L' for the recoverable (assumed linear) part and the superscript 'R' for the remanent part (equivalent to the plastic part in crystalline plasticity), we decompose the total strain ε_{ij} and the total electric displacement D_i into the linear and remanent parts

$$\varepsilon_{ij} = \varepsilon_{ij}^{L} + \varepsilon_{ij}^{R} \tag{2.1a}$$

and

$$D_i = D_i^{L} + P_i^{R} \tag{2.1b}$$

The strain ε_{ij}^{R} is defined as the remanent strain and P_i^{R} is defined as the remanent polarisation, both obtained upon the removal of electrical and mechanical loading (σ_{ij}, E_i). We shall assume that strains remain sufficiently small for infinitesimal theory to apply, with the total strain derived from the displacement field u_i according to

$$\varepsilon_{ij} \equiv \tfrac{1}{2}(u_{i,j}+u_{j,i}) \tag{2.2}$$

The linear response of the ferroelectric solid is given by that of a linear piezoelectric

$$\sigma_{ij} = c^{D}_{ijkl}(\varepsilon_{kl}-\varepsilon^{R}_{kl})-h_{kij}(D_k-P^{R}_{k}) \tag{2.3a}$$

and

$$E_i = -h_{ikl}(\varepsilon_{kl}-\varepsilon^{R}_{kl})+\beta^{\varepsilon}_{ik}(D_k-P^{R}_{k}) \tag{2.3b}$$

where c^{D}_{ijkl} is an elastic stiffness tensor, h_{ijk} is a piezoelectric tensor and β^{ε}_{ij} is a dielectric impermeability tensor. A number of alternative versions of the piezoelectric relations exist, each exactly equivalent to (2.3a,b). For example the above relations can be inverted to give

$$\varepsilon_{ij}-\varepsilon^{R}_{ij} = s^{E}_{ijkl}\sigma_{kl}+d_{kij}E_k \tag{2.4a}$$

and

$$D_i-P^{R}_{i} = d_{ikl}\sigma_{kl}+\kappa^{\sigma}_{ik}E_k \tag{2.4b}$$

Alternatively, $(\sigma_{ij}, D_i-P^{R}_{i})$ is related to $(\varepsilon_{ij}-\varepsilon^{R}_{ij}, E_i)$ by

$$\sigma_{ij} = c^{E}_{ijkl}(\varepsilon_{kl}-\varepsilon^{R}_{kl})-e_{kij}E_k \tag{2.5a}$$

and

$$D_i-P^{R}_{i} = e_{ikl}(\varepsilon_{kl}-\varepsilon^{R}_{kl})+\kappa^{\varepsilon}_{ik}E_k \tag{2.5b}$$

Relations (2.3)–(2.5) remain valid during the non-linear switching of a ferroelectric, but are not sufficient to relate an increment in the loading $(\dot{\sigma}_{ij}, \dot{E}_i)$ to the corresponding increment in configurational quantities $(\dot{\varepsilon}_{ij}, \dot{D}_i)$. A complete framework requires information on how the remanent increments $(\dot{\varepsilon}^{R}_{ij}, \dot{P}^{R}_{i})$ evolve with increments in loading $(\dot{\sigma}_{ij}, \dot{E}_i)$.

Static mechanical equilibrium dictates that the stress σ_{ij} is in equilibrium with an imposed distribution of body force f_i according to

$$\sigma_{ij,j}+f_i = 0 \tag{2.6}$$

and Gauss's law likewise dictates that the divergence of the electric displacement equals the distribution of free charge density q

$$D_{i,i}-q = 0 \tag{2.7}$$

Assuming quasi-static conditions, the electric field is derived from an electric potential Φ via

$$E_i \equiv -\Phi_{,i} \tag{2.8}$$

On the surface S of a piezoelectric body, with unit outward normal n_i, the traction t_i is in equilibrium with the stress σ_{ij} according to

$$t_j = n_i\sigma_{ij} \tag{2.9a}$$

and the surface-free charge density Q is in equilibrium with the jump in electric displacement $\langle D_i \rangle$ across S, such that

$$Q = n_i \langle D_i \rangle = n_i (D_i^o - D_i) \tag{2.9b}$$

Here, we use the symbol $\langle\ \rangle$ to denote the jump in a quantity at the boundary and D_i^o is the electrical displacement exterior to the body. Relations (2.2) and (2.6)–(2.9) have been written in strong form and can equivalently be written in the weak variational form

$$\int_V [\sigma_{ij}\delta\varepsilon_{ij} + E_i \delta D_i]\, \mathrm{d}V = \int_S [t_i \delta u_i + \Phi(\delta Q - n_i \delta D_i^o)]\, \mathrm{d}S + \int_V [f_i \delta u_i + \Phi \delta q]\, \mathrm{d}V \tag{2.10}$$

This variational statement is the fundamental virtual work expression for the solid: the left-hand-side denotes the internal virtual work, the first term on the right-hand-side is the external work done on the external boundary of the solid and the second term on the right-hand-side is the work done by internal body forces. We now proceed to develop a criterion for the progressive switching of a single ferroelectric domain and then generalise to the case of a crystal containing many domains.

3. Switching criterion for a single ferroelectric domain

We adopt the standpoint that domain wall motion gives rise to a progressive change in value of the net remanent polarisation P_i^R and strain ε_{ij}^R for the crystal and is a dissipative process, akin to plastic slip by dislocation motion. Our simplified physical picture of the switching process within a single crystal is shown in Fig. 2, for the case

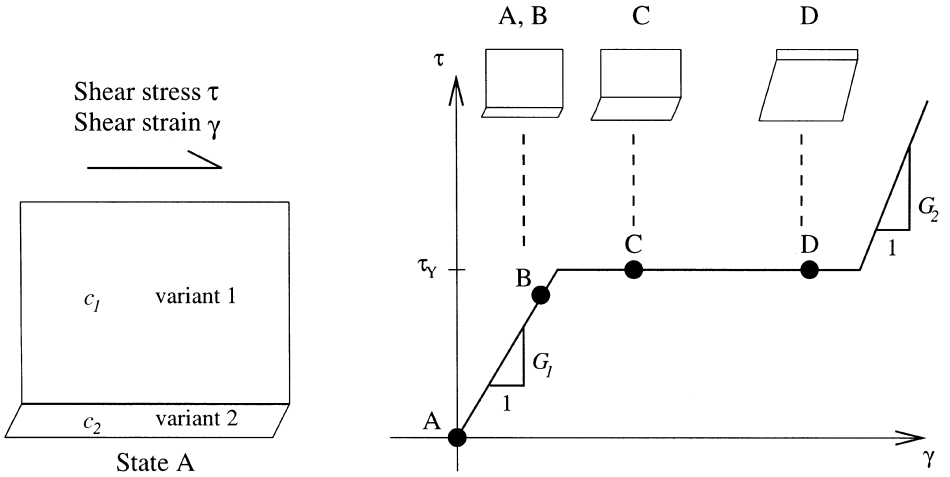

Fig. 2. The progressive nature of ferroelectric transformation within a crystal due to domain wall motion.

of switching between two variants (1) and (2) within the same single crystal, by the motion of a domain wall. In our discussion, we assume the switching event is driven by mechanical stress, but the argument generalises immediately to the purely electrical case and the combined electrical and mechanical case.

The crystal is shown in the initial stress-free state A, with a volume fraction c_1 of variant (1) and a much smaller volume fraction $c_2 = 1 - c_1$ of variant 2. For simplicity, the crystal shown has only two variants present. In reality, single crystals have many domains and walls, but the average effects are the same. The initial elastic shear modulus of the crystal is close to that of variant 1, $G \approx G_1$. Now apply a shear stress τ in a direction which will encourage transformation from variant 1 to 2. At sufficiently low stress levels, the response of the crystal is linear elastic, for example state B of Fig. 2. When τ is increased to a 'yield value' τ_Y, the crystal progressively transforms from variant 1 to 2 by vertical motion of the horizontal domain wall. As the domain wall translates, the average shear strain in the crystal increases and the crystal evolves through states C and D, as shown. It is assumed that domain wall motion is dissipative and only occurs when the driving force τ attains the critical value τ_Y sufficient to provide the dissipated work. The switching event is modelled as the steady-state propagation of an instability, analogous to the propagation of collapse of a pipeline under external pressure, the steady state drawing of a polymer and the motion of a dislocation on a slip plane at constant resolved shear stress, for example. Since the switching process is in steady-state, the critical shear stress is constant.

On continued loading, the crystal switches fully to the variant 2 and the elastic shear modulus attains that of variant 2, $G = G_2$. Additional switching is precluded and the switching process has 'locked-up'. This lock-up phenomenon distinguishes the twinning and switching processes from that of continued plastic glide of a crystal. We note in passing that the Peierls stress for dislocation motion in a perovskite ferroelectric is much greater than the critical resolved shear stress τ_Y for switching to occur; therefore, we neglect the effects of dislocation plasticity. This model carries over directly to the electromechanical case, as described below.

3.1. *Switching criterion for a crystallite and specification of tangent modulus*

In this section, we postulate a switching criterion for a crystallite, analogous to the operation of multiple slip systems in a metallic single crystal. The underlying idea is that switching occurs by the operation of a discrete set of switching systems, whereby one variant converts progressively to another by gradual dissipative domain wall motion. The following assumptions are made to simplify the analysis:

(i) The stress σ_{ij} and the electric field E_i are uniform in the crystal.
(ii) The crystal has a volume fraction c^I of each variant I. For a tetragonal crystal, there are a total of $M = 6$ variants.
(iii) Both the linear and the remanent parts of the strain ε_{ij} and the electric displacement D_i are given by the volume averages over the crystal.

In general, each variant I within a crystal is assumed to possess anisotropic linear electromechanical properties specified by the mechanical compliancies $s_{ijkl}^{E(I)}$, pie-

zoelectric coefficients $d_{ijk}^{(I)}$ and dielectric permittivities $\kappa_{ij}^{\sigma(I)}$, such that the linear strain $\varepsilon_{ij}^{L(I)}$ and the linear electric displacement $D_i^{L(I)}$ in variant I are given by

$$\varepsilon_{ij}^{L(I)} = s_{ijkl}^{E(I)}\sigma_{kl} + d_{kij}^{(I)}E_k \tag{3.1a}$$

and

$$D_i^{L(I)} = d_{ikl}^{(I)}\sigma_{kl} + \kappa_{ik}^{\sigma(I)}E_k \tag{3.1b}$$

Then, by assumption (iii), the average linear strain and electric displacement in the crystal is

$$\varepsilon_{ij}^{L} = \sum_{I=1}^{I=M} [c^I \varepsilon_{ij}^{L(I)}] = s_{ijkl}^{E}\sigma_{kl} + d_{kij}E_k \tag{3.2a}$$

and

$$D_i^{L} = \sum_{I=1}^{I=M} [c^I D_i^{L(I)}] = d_{ikl}\sigma_{kl} + \kappa_{ik}^{\sigma}E_k \tag{3.2b}$$

where

$$s_{ijkl}^{E} = \sum_{I=1}^{I=M} [c^I s_{ijkl}^{E(I)}] \tag{3.3a}$$

$$d_{ijk} = \sum_{I=1}^{I=M} [c^I d_{ijk}^{(I)}] \tag{3.3b}$$

$$\kappa_{ij}^{\sigma} = \sum_{I=1}^{I=M} [c^I \kappa_{ij}^{\sigma(I)}] \tag{3.3c}$$

The incremental remanent strain and polarisation $(\dot{\varepsilon}_{ij}^{R}, \dot{P}_i^{R})$ are determined as follows. Consider transformation between different variants. Each of the M variants can transform into any of the remaining $(M-1)$ variants, giving a total of $N = M(M-1)$ transformations. (For the case of tetragonal crystals with six variants there exists a total of 30 possible transformations, comprising 90° and 180° switches.) Each transformation α is characterised by a transformation strain of magnitude γ^{α} which is the difference in spontaneous strain between the two variants involved and by a transformation electric polarisation of magnitude P^{α} which is the difference in electric polarisation.

3.2. *Kinematics*

A change in volume fraction c^I of the variant I is by activation of a number of transformation systems α. Left $\dot{f}^{\alpha}$ denote the incremental volume fraction of material transformed from a variant J to a variant I. For book-keeping purposes we introduce a connectivity matrix $A^{I\alpha}$ such that $A^{I\alpha} = 1$ if activation of the transformation system α increases the volume fraction c^I of variant I, $A^{I\alpha} = -1$ if activation of the system α

depletes the volume fraction c^I of variant I and $A^{I\alpha} = 0$ if operation of the transformation system α does not change the volume fraction c^I. Thus, $A^{I\alpha}$ is a $M \times N$ matrix and connects $\dot{f}^\alpha$ to $\dot{c}^I$ according to

$$\dot{c}^I = \sum_{\alpha=1}^{N} A^{I\alpha}\dot{f}^\alpha, \quad I = 1, 2, \ldots, M \tag{3.4}$$

Next, we obtain an expression for the remanent strain rate $\dot{\varepsilon}_{ij}^R$ and the remanent electric polarisation rate $\dot{P}_i^R$ in terms of the transformation rate $\dot{f}^\alpha$. The transformation rate $\dot{f}^\alpha$ produces a remanent strain increment in the crystal of $\dot{f}^\alpha \mu_{ij}^\alpha \gamma^\alpha$, where μ_{ij}^α is the unit orientation tensor for the transformation system α, defined as follows. Transformation is by simple shear in a direction s_i^α on a plane of unit normal n_i^α. Hence, the usual Schmid orientation tensor μ_{ij}^α is defined by

$$\mu_{ij}^\alpha = \tfrac{1}{2}(s_i^\alpha n_j^\alpha + s_j^\alpha n_i^\alpha) \tag{3.5}$$

Simultaneously the transformation rate $\dot{f}^\alpha$ produces a remanent polarisation increment in the crystal of $\dot{f}^\alpha s_i^\alpha P^\alpha$. If several transformation systems are active simultaneously, then the remanent strain and polarisation increments are computed by summing over all active systems, giving

$$\dot{\varepsilon}_{ij}^R = \sum_\alpha \dot{f}^\alpha \mu_{ij}^\alpha \gamma^\alpha \tag{3.6a}$$

and

$$\dot{P}_i^R = \sum_\alpha \dot{f}^\alpha s_i^\alpha P^\alpha \tag{3.6b}$$

Note that the quantities $\dot{f}^\alpha$ are the fundamental kinematic variables of the transformation process and couple the increments of remanent strain and polarisation. We will adopt the convention that $\dot{f}^\alpha$ is never negative and thereby, in effect, double the number of transformation systems.

3.3. *Driving force for each transformation system*

We shall derive a transformation criterion for the operation of each transformation system analogous to a yield criterion for operation of a slip system in crystal plasticity theory. The driving force for each of the transformation systems is defined as the work conjugate to the rate of change of volume fraction of the variants $\dot{f}^\alpha$ and is derived by writing the overall dissipative work rate per unit volume $\dot{w}^D$ of the crystal in terms of the work rate for each transformation system. First, we define the dissipative work rate $\dot{w}^D$ as the total work rate $\dot{w}$ minus the recoverably stored electromechanical work rate, $\dot{w}^S$, giving

$$\dot{w}^D = \dot{w} - \dot{w}^S = \sigma_{ij}\dot{\varepsilon}_{ij} + E_i\dot{D}_i - \dot{w}^S \tag{3.7}$$

where the recoverably stored electromechanical energy w^S is expressed by

$$w^S = \tfrac{1}{2}\sigma_{ij}(\varepsilon_{ij} - \varepsilon_{ij}^R) + \tfrac{1}{2}E_i(D_i - P_i^R) \tag{3.8}$$

Upon making use of (2.3) and (3.1)–(3.4), the stored electromechanical work rate $\dot{w}^S$ follows as

$$\dot{w}^S = \sigma_{ij}(\dot{\varepsilon}_{ij} - \dot{\varepsilon}_{ij}^R) + E_i(\dot{D}_i - \dot{P}_i^R) - \sum_\alpha \left[\frac{1}{2}\sigma_{ij}\tilde{\varepsilon}_{ij}^\alpha + \frac{1}{2}E_i\tilde{D}_i^\alpha\right]\dot{f}^\alpha \tag{3.9}$$

where

$$\tilde{\varepsilon}_{ij}^\alpha \equiv \sum_I A^{I\alpha}[s_{ijkl}^{E(I)}\sigma_{kl} + d_{kij}^{(I)}E_k] \tag{3.10a}$$

and

$$\tilde{D}_i^\alpha \equiv \sum_I A^{I\alpha}[d_{ikl}^{(I)}\sigma_{kl} + \kappa_{ik}^{\sigma(I)}E_k] \tag{3.10b}$$

Substitution of the expression (3.9) for $\dot{w}^S$ into (3.7) gives an explicit expression for $\dot{w}^D$

$$\dot{w}^D = \sigma_{ij}\dot{\varepsilon}_{ij}^R + E_i\dot{P}_i^R + \sum_\alpha \left[\frac{1}{2}\sigma_{ij}\tilde{\varepsilon}_{ij}^\alpha + \frac{1}{2}E_i\tilde{D}_i^\alpha\right]\dot{f}^\alpha \tag{3.11}$$

On defining the resolved shear stress τ^α on transformation system α by

$$\tau^\alpha = \sigma_{ij}\mu_{ij}^\alpha \tag{3.12a}$$

and the resolved electric field E^α on transformation system α by

$$E^\alpha = E_i s_i^\alpha \tag{3.12b}$$

the dissipative work rate (3.11) simplifies to the form

$$\dot{w}^D = \sum_\alpha [G^\alpha \dot{f}^\alpha] \tag{3.12c}$$

where G^α is the driving force for transformation and is defined by

$$G^\alpha = \tau^\alpha\gamma^\alpha + E^\alpha P^\alpha + \tfrac{1}{2}\sigma_{ij}\tilde{\varepsilon}_{ij}^\alpha + \tfrac{1}{2}E_i\tilde{D}_i^\alpha \quad \text{(no sum on } \alpha) \tag{3.13}$$

It is natural to view G^α as the thermodynamic driving force for transformation; equally, it can be viewed as the energy dissipated by domain wall motion upon transforming a unit volume of crystal from one variant to the next by operation of the transformation system α. The transformation system α is taken to be potentially active when G^α attains the critical value G_c^α considered to be characteristic of the dissipation caused by domain wall motion. The potentially active system loads when

$$G^\alpha = G_c^\alpha \quad \text{and} \quad \dot{G}^\alpha = \dot{G}_c^\alpha \quad \text{with } \dot{f}^\alpha \geqslant 0 \tag{3.14a}$$

and unloads when

$$G^\alpha = G_c^\alpha \quad \text{and} \quad \dot{G}^\alpha < \dot{G}_c^\alpha \quad \text{with } \dot{f}^\alpha = 0 \tag{3.14b}$$

A system is inactive if $G^\alpha < G_c^\alpha$ and then $\dot{f}^\alpha = 0$.

In the absence of work-hardening, the quantities G_c^α are taken to be constant. Here, we follow Hill (1966) and assume that hardening can occur and is described by

$$\dot{G}_c^\alpha = \sum_\beta H^{\alpha\beta} \dot{f}^\beta \tag{3.15}$$

where the summation is taken over all active transformation systems and $H^{\alpha\beta}$ is the hardening matrix. For the case of progressive ferroelectric transformation, we argue on physical grounds that the degree of hardening is negligible and so we introduce the matrix $H^{\alpha\beta}$ to regularise the computation, rather than for physical reasons. In this initial study we assume independent hardening, with $\boldsymbol{H} = H\boldsymbol{I}$, where $\boldsymbol{I}$ is the unit matrix. The scalar H is taken to be sufficiently small in order to reproduce numerically results for the perfectly plastic case (as specified in Section 5). In the limit $H^{\alpha\beta} \to 0$ the constitutive response is independent of the precise choice of hardening matrix. This approach is similar to that used in the modelling of slip in elastic–perfectly plastic crystals.

The switching surface at each material point in combined (σ_{ij}, E_i) space consists of a set of planes defined by $G^\alpha = G_c^\alpha$ for all transformation systems α. Each transformation system satisfies

$$(G^\alpha - G^{\alpha *})\dot{f}^\alpha \geqslant 0 \tag{3.16}$$

for a driving force $G^\alpha = G_c^\alpha$ corresponding to a transformation rate $\dot{f}^\alpha$ and for any alternative driving force $G^{\alpha *}$ less than or equal to the critical value G_c^α. Then, by (3.11)–(3.13), the stress, electric field, strain rate and electric displacement rate satisfy

$$(\sigma_{ij} - \sigma_{ij}^*)\dot{\varepsilon}_{ij}^R + (E_i - E_i^*)\dot{P}_i^R \geqslant -\sum_\alpha \left[\frac{1}{2}(\sigma_{ij}\tilde{\varepsilon}_{ij}^\alpha + E_i\tilde{D}_{ij}^\alpha - \sigma_{ij}^*\tilde{\varepsilon}_{ij}^{*\alpha} - E_i^*\tilde{D}_i^{*\alpha})\dot{f}^\alpha\right] \tag{3.17}$$

for a state (σ_{ij}, E_i) associated with a remanent rate $(\dot{\varepsilon}_{ij}^R, \dot{P}_i^R)$ and for a neighbouring state (σ_{ij}^*, E_i^*) on or within the yield surface. If the right-hand-side of (3.17) were to vanish then the switching surface would be convex and the remanent rate $(\dot{\varepsilon}_{ij}^R, \dot{P}_i^R)$ would be normal to the switching surface. In general, this is not the case and we assert neither convexity nor normality.

3.4. *Tangent moduli for a crystal*

Our constitutive formulation is written in incremental form, with the tangent moduli for a crystal defined via

$$\begin{pmatrix} \dot{\sigma}_{ij} \\ \dot{E}_i \end{pmatrix} = \begin{bmatrix} c_{ijkl}^{D,t} & -h_{kij}^t \\ -h_{ikl}^t & \beta_{ik}^{\varepsilon,t} \end{bmatrix} \begin{pmatrix} \dot{\varepsilon}_{kl} \\ \dot{D}_k \end{pmatrix} \tag{3.18}$$

The tangent stiffnesses ($c_{ijkl}^{D,t}$, h_{ijk}^t and $\beta_{ij}^{\varepsilon,t}$) are now derived. Time differentiation of the linear relations (3.2a,b) and use of (3.3) and (3.4) gives

$$\dot{\varepsilon}_{ij} - \dot{\varepsilon}^R_{ij} = s^E_{ijkl}\dot{\sigma}_{kl} + d_{kij}\dot{E}_k + \sum_\alpha \tilde{\varepsilon}^\alpha_{ij}\dot{f}^\alpha \tag{3.19a}$$

and

$$\dot{D}_i - \dot{P}^R_i = d_{ikl}\dot{\sigma}_{kl} + \kappa^\sigma_{ik}\dot{E}_k + \sum_\alpha \tilde{D}^\alpha_i \dot{f}^\alpha \tag{3.19b}$$

The summation terms on the right-hand-side of (3.19a,b) are the linear strain and electric displacement contributions associated with a change in linear electromechanical properties with phase transformation. In order to construct the tangent stiffnesses, we invert (3.19a,b) and make use of (2.1a,b) and (3.6a,b), to obtain

$$\begin{pmatrix}\dot{\sigma}_{ij}\\ \dot{E}_i\end{pmatrix} = \begin{bmatrix} c^D_{ijkl} & -h_{kij} \\ -h_{ikl} & \beta^\varepsilon_{ik}\end{bmatrix}\left(\begin{pmatrix}\dot{\varepsilon}_{kl}\\ \dot{D}_k\end{pmatrix} - \sum_\alpha \begin{pmatrix}\hat{\varepsilon}^\alpha_{kl}\\ \hat{D}^\alpha_k\end{pmatrix}\dot{f}^\alpha\right) \tag{3.20}$$

where

$$\hat{\varepsilon}^\alpha_{kl} \equiv \mu^\alpha_{kl}\dot{\gamma}^\alpha + \tilde{\varepsilon}^\alpha_{kl} \tag{3.21a}$$

and

$$\hat{D}^\alpha_k \equiv s^\alpha_k P^\alpha + \tilde{D}^\alpha_k \tag{3.21b}$$

To proceed, we relate the rate quantities $(\dot{\varepsilon}_{ij}, \dot{D}_i)$ to the volume fraction increments $\dot{f}^\alpha$ by making use of hardening rule (3.15), expressed in terms of stress and electric field rates. Recall that the driving force G^α is related to the mechanical stress and the electric field via (3.12a,b) and (3.13). Then, in incremental form, for active transformation systems α

$$\dot{G}^\alpha = \dot{G}^\alpha_c = \dot{\sigma}_{ij}\hat{\varepsilon}^\alpha_{ij} + \dot{E}_k\hat{D}^\alpha_k \tag{3.22}$$

The hardening rule (3.15) provides the pivotal connection between the stress rates given in (3.22) and the strain rates given in (3.20), so that

$$\sum_\beta H^{\alpha\beta}\dot{f}^\beta = \dot{G}^\alpha_c = (\hat{\varepsilon}^\alpha_{ij} \quad \hat{D}^\alpha_i)\begin{bmatrix} c^D_{ijkl} & -h_{kij} \\ -h_{ikl} & \beta^\varepsilon_{ik}\end{bmatrix}\left(\begin{pmatrix}\dot{\varepsilon}_{kl}\\ \dot{D}_k\end{pmatrix} - \sum_\beta \begin{pmatrix}\hat{\varepsilon}^\beta_{kl}\\ \hat{D}^\beta_k\end{pmatrix}\dot{f}^\beta\right) \tag{3.23}$$

Note that α and β range over the set of active transformation systems in eqn (3.23). Rearrangement of this relation gives

$$\dot{f}^\alpha = \sum_\beta [(X^{\alpha\beta})^{-1}(\hat{\varepsilon}^\beta_{ij} \quad \hat{D}^\beta_i)]\begin{bmatrix} c^D_{ijkl} & -h_{kij} \\ -h_{ikl} & \beta^\varepsilon_{ik}\end{bmatrix}\begin{pmatrix}\dot{\varepsilon}_{kl}\\ \dot{D}_k\end{pmatrix} \tag{3.24}$$

where

$$X^{\alpha\beta} \equiv H^{\alpha\beta} + (\hat{\varepsilon}^\alpha_{ij} \quad \hat{D}^\alpha_i)\begin{bmatrix} c^D_{ijkl} & -h_{kij} \\ -h_{ikl} & \beta^\varepsilon_{ik}\end{bmatrix}\begin{pmatrix}\hat{\varepsilon}^\beta_{kl}\\ \hat{D}^\beta_k\end{pmatrix} \tag{3.25}$$

Here, $(X^{\alpha\beta})^{-1}$ denotes the inverse of the matrix $X^{\alpha\beta}$, which is assumed to be non-singular. Equation (3.24) gives an explicit expression for the increments in volume fraction $\dot{f}^{\alpha}$ in terms of the increments of strain and electric displacement and it is convenient to write it in the simpler form

$$\dot{f}^{\alpha} = \sum_{\beta} [(X^{\alpha\beta})^{-1} (\hat{\sigma}_{ij}^{\beta} \dot{\varepsilon}_{ij} + \hat{E}_i^{\beta} \dot{D}_i)] \tag{3.26}$$

where

$$\hat{\sigma}_{ij}^{\beta} \equiv c_{ijkl}^{D} \hat{\varepsilon}_{kl}^{\beta} - h_{kij} \hat{D}_k^{\beta} \tag{3.27a}$$

and

$$\hat{E}_i^{\beta} \equiv -h_{ijk} \hat{\varepsilon}_{jk}^{\beta} + \beta_{ij}^{\varepsilon} \hat{D}_j^{\beta} \tag{3.27b}$$

The final step in finding the tangent properties of the crystal is to substitute the expression for $\dot{f}^{\alpha}$ back into (3.20), giving the form (3.18) with

$$c_{ijkl}^{D,t} = c_{ijkl}^{D} - \sum_{\alpha} \sum_{\beta} [\hat{\sigma}_{ij}^{\alpha} (X^{\alpha\beta})^{-1} \hat{\sigma}_{kl}^{\beta}] \tag{3.28a}$$

$$\begin{aligned} h_{kij}^{t} &= h_{kij} + \sum_{\alpha} \sum_{\beta} [\hat{\sigma}_{ij}^{\alpha} (X^{\alpha\beta})^{-1} \hat{E}_k^{\beta}] \\ &= h_{kij} + \sum_{\alpha} \sum_{\beta} [\hat{E}_k^{\alpha} (X^{\alpha\beta})^{-1} \hat{\sigma}_{ij}^{\beta}] \end{aligned} \tag{3.28b}$$

and

$$\beta_{ij}^{\varepsilon,t} = \beta_{ij}^{\varepsilon} - \sum_{\alpha} \sum_{\beta} [\hat{E}_i^{\alpha} (X^{\alpha\beta})^{-1} \hat{E}_j^{\beta}] \tag{3.28c}$$

The introduction of the notation $\hat{\sigma}_{ij}^{\alpha}$ with dimensions of stress and $\hat{E}_i^{\alpha}$ with dimensions of electric field reveals both the dimensionalities and symmetries of the tangent moduli. Note that $c_{ijkl}^{D,t}$, h_{ijk}^{t} and $\beta_{ij}^{\varepsilon,t}$ have Cauchy-type symmetries if $X^{\alpha\beta}$, and hence $H^{\alpha\beta}$, is symmetric. We have assumed that $H^{\alpha\beta}$ is symmetric and therefore all of the tangent properties (3.28a–c) have Cauchy-type symmetries and allow for the existence of a rate potential, $U(\dot{\boldsymbol{\varepsilon}}, \dot{\boldsymbol{D}})$, where

$$U(\dot{\boldsymbol{\varepsilon}}, \dot{\boldsymbol{D}}) = \tfrac{1}{2} \dot{\sigma}_{ij} \dot{\varepsilon}_{ij} + \tfrac{1}{2} \dot{E}_i \dot{D}_i = \tfrac{1}{2} c_{ijkl}^{D,t} \dot{\varepsilon}_{ij} \dot{\varepsilon}_{kl} - h_{kij}^{t} \dot{D}_k \dot{\varepsilon}_{ij} + \tfrac{1}{2} \beta_{ij}^{\varepsilon,t} \dot{D}_i \dot{D}_j \tag{3.29}$$

such that

$$\dot{\sigma}_{ij} = \frac{\partial U}{\partial \dot{\varepsilon}_{ij}} \quad \text{and} \quad \dot{E}_i = \frac{\partial U}{\partial \dot{D}_i} \tag{3.30}$$

The rate potential U is homogeneous of degree 2 in $(\dot{\varepsilon}_{ij}, \dot{D}_{ij})$, but is not necessarily convex. Therefore, uniqueness of $(\dot{\sigma}_{ij}, \dot{E}_{ij})$ is not guaranteed for a given $(\dot{\varepsilon}_{ij}, \dot{D}_k)$ and a minimum principle for the rate boundary value problem cannot be constructed along the lines of Hill (1966). However, a stationary variational principle can be stated as follows. Consider a polycrystal of volume V and surface S, comprised of ferroelectric

crystals each with constitutive law (3.18)–(3.30). The body is loaded by the instantaneous traction rate $\dot{t}_i^o$ and electric potential rate $\dot{\Phi}^o$ on a portion S_T of its surface. The velocity $\dot{u}_i$ and the rate of accumulation of surface free charge density $(\dot{Q}-n_i\dot{D}_i^o)$ are given on the remaining portion S_u of the surface. Consider all possible velocity fields $\dot{u}_i$ and electric displacement rate fields $\dot{D}_i$ within V, which satisfy the kinematic conditions on S_u and define $(\dot{\sigma}_{ij}, \dot{E}_i)$ to be given by the constitutive law (3.18)–(3.30). Then, the functional $F(\dot{u}_i, \dot{D}_i)$, defined by

$$F(\dot{u}_i, \dot{D}_i) \equiv \int_V U(\dot{\varepsilon}_{ij}, \dot{D}_k)\,\mathrm{d}V - \int_{S_T} [\dot{t}_i^o \dot{u}_i + \dot{\mathbf{\Phi}}^o(\dot{Q}-n_i\dot{D}_i^o)]\,\mathrm{d}S \tag{3.31}$$

is stationary about the solution for the rate problem. The first variation of F gives the rate form of the virtual work statement (2.10). Dual functionals in $(\dot{\sigma}_{ij}, \dot{E}_i)$ can likewise be constructed, but are omitted here for the sake of brevity.

4. Self-consistent scheme for the polycrystal

We shall consider the non-linear response of a polycrystal by extending the self-consistent scheme developed by Hill (1965a, b). Macroscopic rates of stress and electric field, $(\dot{\bar{\sigma}}_{ij}, \dot{\bar{E}}_i)$ and rates of strain and electric displacement, $(\dot{\bar{\varepsilon}}_{ij}, \dot{\bar{D}}_i)$, for the polycrystal are defined as the volume averages of the rate quantities in the single crystals. For the purely mechanical case, Hill (1967) has shown that the definition in terms of strain quantities is rigorously consistent for a finite collection of single crystals under either a prescribed uniform surface traction over the boundary, or a prescribed 'uniform straining' of the boundary surface. If the polycrystal comprises a sufficiently large number of crystals, the distinction between these two ways of prescribing the loading is negligible. The generalisation of these statements to the combined electromechanical case is immediate. For conceptual simplicity, we shall view the polycrystal as an infinite collection of single crystals subject to macroscopically homogeneous states of $(\bar{\sigma}_{ij}, \bar{E}_i)$ and $(\bar{\varepsilon}_{ij}, \bar{D}_i)$. We assume that no free charge is present in the interior of the polycrystal.

We suppose that the polycrystal has undergone some definite history of loading and that the current state of stress and electric field and the potentially active transformation systems in each crystal are known. The polycrystal is subjected to a prescribed macroscopic strain rate and electric displacement rate, $(\dot{\bar{\varepsilon}}_{ij}, \dot{\bar{D}}_i)$. Our objective is to calculate the rates $(\dot{\varepsilon}_{ij}, \dot{D}_i)$ and $(\dot{\sigma}_{ij}, \dot{E}_i)$ within each crystal, as well as the instantaneous tangent moduli for each crystal and thereby to determine the macroscopic polycrystalline quantities $(\dot{\bar{\sigma}}_{ij}, \dot{\bar{E}}_i)$ and the overall tangent moduli as the appropriate averages over the grains. In order to explain the self-consistent scheme for calculation of the overall, macroscopic quantities, it is assumed that the active transformation systems and the associated tangent moduli in each grain are known for each grain.

We extend the scheme of Hill (1965a, b) to calculate the macroscopic rates $(\dot{\bar{\sigma}}_{ij}, \dot{\bar{E}}_i)$ for a prescribed $(\dot{\bar{\varepsilon}}_{ij}, \dot{\bar{D}}_i)$. We seek the values of the overall tangent moduli $(c_{ijkl}^{D,o}, h_{kij}^o, \beta_{ik}^{\varepsilon,o})$ defined by

$$\begin{pmatrix} \dot{\bar{\sigma}}_{ij} \\ \dot{\bar{E}}_i \end{pmatrix} = \begin{bmatrix} c^{D,o}_{ijkl} & -h^{o}_{kij} \\ -h^{o}_{ikl} & \beta^{\varepsilon,o}_{ik} \end{bmatrix} \begin{pmatrix} \dot{\bar{\varepsilon}}_{kl} \\ \dot{\bar{D}}_k \end{pmatrix} \tag{4.1}$$

First, we obtain the relation between the macroscopic strain and electric displacement rates and the average strain and electric displacement rates in each crystal. The connections between the stress rate in each crystal $\dot{\sigma}_{ij}$ and the average stress rate for the polycrystal $\dot{\bar{\sigma}}_{ij}$, (and between $\dot{E}_i$ and $\dot{\bar{E}}_i$) are given by constraint tensors as

$$\begin{pmatrix} \dot{\sigma}_{ij} - \dot{\bar{\sigma}}_{ij} \\ \dot{E}_i - \dot{\bar{E}}_i \end{pmatrix} = -\begin{bmatrix} c^{D^*}_{ijkl} & -h^{*}_{kij} \\ -h^{*}_{ikl} & \beta^{\varepsilon^*}_{ik} \end{bmatrix} \begin{pmatrix} \dot{\varepsilon}_{kl} - \dot{\bar{\varepsilon}}_{kl} \\ \dot{D}_k - \dot{\bar{D}}_k \end{pmatrix} \tag{4.2}$$

The constraint tensors $(c^{D^*}_{ijkl}, h^{*}_{kij}, \beta^{\varepsilon^*}_{ik})$ are given in Appendix A. On using (3.18) and (4.1) to eliminate $(\dot{\sigma}_{ij}, \dot{E}_i)$ and $(\dot{\bar{\sigma}}_{ij}, \dot{\bar{E}}_i)$ from (4.2), we obtain

$$\begin{bmatrix} c^{D,t}_{ijkl} + c^{D^*}_{ijkl} & -h^{t}_{kij} - h^{*}_{kij} \\ -h^{t}_{ikl} - h^{*}_{ikl} & \beta^{\varepsilon,t}_{ik} + \beta^{\varepsilon^*}_{ik} \end{bmatrix} \begin{pmatrix} \dot{\varepsilon}_{kl} \\ \dot{D}_k \end{pmatrix} = \begin{bmatrix} c^{D,o}_{ijkl} + c^{D^*}_{ijkl} & -h^{o}_{kij} - h^{*}_{kij} \\ -h^{o}_{ikl} - h^{*}_{ikl} & \beta^{\varepsilon,o}_{ik} + \beta^{\varepsilon^*}_{ik} \end{bmatrix} \begin{pmatrix} \dot{\bar{\varepsilon}}_{kl} \\ \dot{\bar{D}}_k \end{pmatrix} \tag{4.3}$$

which may be rearranged to the form

$$\begin{pmatrix} \dot{\varepsilon}_{ij} \\ \dot{D}_i \end{pmatrix} = \begin{bmatrix} A^{\varepsilon\varepsilon}_{ijkl} & A^{\varepsilon D}_{kij} \\ A^{D\varepsilon}_{ikl} & A^{DD}_{ik} \end{bmatrix} \begin{pmatrix} \dot{\bar{\varepsilon}}_{kl} \\ \dot{\bar{D}}_k \end{pmatrix} \tag{4.4}$$

thereby defining the A-tensors. The A-tensors have the physical interpretation that they relate the average strain rate (and average electric displacement rate) in each crystal to the macroscopic strain rate (and macroscopic electric displacement rate); they generalise the A-tensor introduced by Hill (1965a, b).

Second, we average (3.18) over the polycrystal and use (4.4) to obtain an explicit expression for the tangent moduli of the polycrystal (4.1), with

$$c^{D,o}_{ijkl} = \overline{c^{D,t}_{ijrs} A^{\varepsilon\varepsilon}_{rskl} - h^{t}_{rij} A^{D\varepsilon}_{rkl}} \tag{4.5a}$$

$$h^{o}_{kij} = \overline{-c^{D,t}_{ijrs} A^{\varepsilon D}_{krs} + h^{t}_{rij} A^{DD}_{rk}}$$

$$= \overline{h^{t}_{krs} A^{\varepsilon\varepsilon}_{rsij} - \beta^{\varepsilon,t}_{kr} A^{D\varepsilon}_{rij}} \tag{4.5b}$$

and

$$\beta^{\varepsilon,o}_{ik} = \overline{-h^{t}_{irs} A^{\varepsilon D}_{krs} + \beta^{\varepsilon,t}_{ir} A^{DD}_{rk}} \tag{4.5c}$$

where an overbar indicates a volume average over all crystals.

5. Self-consistent estimates of polycrystal behaviour

Using the results of Section 4 it is possible to make self-consistent estimates of the incremental response of a ferroelectric polycrystal to any path of macroscopic loading (σ_{ij}, E_i). The numerical procedure adopted here is summarised as follows (see Hutch-

inson, 1970 and Huber, 1998 for additional details). The macroscopic load (σ_{ij}, E_i) is applied incrementally and for each load step a self-consistent estimate of the current tangent properties is used to update (ε_{ij}, D_i).

At the beginning of each load step, the stress, electric field and the volume fraction of each variant within each crystal are known. As a first guess for the current tangent properties of each crystal, it is assumed that all potentially active transformation systems are active. Iteration is used to obtain converged values for the overall tangent properties as defined by (4.5) and for the A-tensors as defined by (4.3) and (4.4). During this iteration, we check that the transformation rate $\dot{f}^{\alpha}$ for each of the active transformation systems satisfies $\dot{f}^{\alpha} \geqslant 0$. Where this condition is not met, the transformation system is taken to be inactive in the next iteration. It is emphasised that this iterative scheme is highly implicit since the tangent properties depend on the set of active transformation systems and vice versa. Nevertheless, the scheme converges rapidly.

The results presented here are calculated for a polycrystal consisting of single crystals with properties corresponding (roughly) to tetragonal lead titanate. All results have been normalised by the parameters τ_0, γ_0, E_0 and D_0. These correspond, respectively, to the shear stress when switching commences under pure shear loading, the shear strain when switching commences under pure shear loading, the electric field when switching commences under pure electric field loading and the electric displacement when switching commences under pure electric field loading. Each tetragonal crystal has six crystal variants corresponding to six polarisation directions which are aligned with the ± 1, ± 2 and ± 3 local crystallographic axes. For simplicity, the initial state for each crystal is chosen to be that with an equal volume fraction (1/6) of each crystal variant. This gives rise to a state of zero average initial remanent strain and polarisation in each crystal. The initial state of stress and electric field in each crystal is set to zero. The crystals are assumed to be non-hardening, but for a small hardening rate to regularise the calculation. Specifically, the value of the scalar hardening modulus H is taken to be 1% of the initial value of G_c^{α} for a 90° switch.

The orientations of the crystallographic axes for the crystals are defined by sets of three Euler angles for each crystal, chosen in such a way that the distribution of polarisation vector directions present initially in the polycrystal is a uniform spherical distribution, Huber (1998). A total of 205 crystals (1230 ferroelectric domains) were modelled. In each single domain region, isotropic linear elasticity and linear dielectric behaviour is assumed, with a piezoelectric tensor corresponding to 4 mm symmetry (Nye, 1957). Thus, in each domain we have

$$c^E_{ijkl} = \frac{2\mu v}{(1-2v)}\delta_{ij}\delta_{kl} + \mu(\delta_{ik}\delta_{jl} + \delta_{il}\delta_{jk})$$

$$d_{ijk} = d_{333}n_in_jn_k + d_{311}(n_i\delta_{jk} - n_in_jn_k) + \tfrac{1}{2}d_{131}(\delta_{ij}n_k - 2n_in_jn_k + \delta_{ik}n_j)$$

and

$$\kappa^{\sigma}_{ik} = \kappa\delta_{ik} \tag{5.1}$$

where n_i is the unit vector in the polarisation direction and specific values for the material parameters are given in Table 1.

Two further assumptions are made here. First, when the constitutive equations (2.3) are normalised, the following expressions are obtained:

$$\frac{\sigma_{ij}}{\tau_0} = \left(\frac{\gamma_0 c^D_{ijkl}}{\tau_0}\right)\frac{(\varepsilon_{kl}-\varepsilon^R_{kl})}{\gamma_0} - \left(\frac{D_0 h_{kij}}{\tau_0}\right)\frac{(D_k - P^R_k)}{D_0} \tag{5.2a}$$

$$\frac{E_i}{E_0} = -\left(\frac{\gamma_0 h_{ikl}}{E_0}\right)\frac{(\varepsilon_{kl}-\varepsilon^R_{kl})}{\gamma_0} + \left(\frac{D_0 \beta^{\varepsilon}_{ik}}{E_0}\right)\frac{(D_k - P^R_k)}{D_0} \tag{5.2b}$$

It is convenient to set the cross terms in eqns (5.2) equal, giving rise to:

$$\tau_0 \gamma_0 = E_0 D_0 \tag{5.3}$$

This represents a physical assumption about the yield condition and is equivalent to the statement that the strain energy density at yield under purely mechanical loading equals the strain energy density at yield under purely electrical loading.

Second, it is necessary to specify the critical value of the driving force for transformation G^α_c for each transformation system α. Note that the hardening rate is chosen to be small such that G^α_c is almost constant for each transformation system. We assume that G^α_c has one value $G^\alpha_c(90^\circ)$ for the 90° transformation systems and another value $G^\alpha_c(180^\circ)$ for the 180° transformation systems. However, it is unclear whether it is physically realistic to assume that $G^\alpha_c(90^\circ) = G^\alpha_c(180^\circ)$. Imposition of this equality would give rise to switching at different magnitudes of electric field for 90° and 180° systems. An alternative assumption is to set the magnitude of the critical electric field to be the same for the 90° and 180° transformations which gives rise to:

$$G^\alpha_c(90^\circ) = G^\alpha_c(180^\circ)/\sqrt{2} \tag{5.4}$$

We shall assume that (5.4) holds for the initial set of simulations presented below. Equations (5.3) and (5.4), together with the constants listed in Table 1 provide sufficient information to specify all of the modelling parameters E_0, τ_0, D_0, γ_0, $G^\alpha_c(90^\circ)$, $G^\alpha_c(180^\circ)$, $\gamma^\alpha(90^\circ)$, $P^\alpha(90^\circ)$ and $P^\alpha(180^\circ)$.

Now consider a loading path consisting of cycling electric field E_3 in the three-

Table 1
Crystal constants

Shear modulus μ [N m^{-2}]	52.6×10^{9}
Poisson's ratio ν [—]	0.22
Dielectric permittivity κ [F m^{-1}]	2.13×10^{-9}
Piezoelectric coefficient d_{333} [m V^{-1}]	56×10^{-12}
Piezoelectric coefficient $d_{311}=d_{322}$ [m V^{-1}]	-6.8×10^{-12}
Piezoelectric coefficient $d_{131}=d_{113}=d_{232}=d_{223}$ [m V^{-1}]	68×10^{-12}
Electric field at yield E_0 [V m^{-1}]	6.75×10^{5}
Polarisation change of transformation system $P^\alpha(180^\circ)/D_0$ [—]	10

direction. Initially, each crystal has zero net remanent strain, polarisation and piezoelectric effect. Similarly, the polycrystal has zero initial remanent strain, polarisation and piezoelectric effect. The polycrystal gives a linear dielectric response up to the point $E_3/E_0 = 1$, $D_3/D_0 = 1$. At this stage the remanent strain is still zero and the linear part of the strain is also zero, because of the absence of a net piezoelectric effect. Beyond this level of loading, ferroelectric transformation occurs, giving rise to the dielectric hysteresis and butterfly hysteresis curves shown in Fig. 3. At the onset of non-linearity, there is a rapid increase in electric displacement due to the appearance of remanent polarisation; similarly, there is an increase in strain due to remanent strain and also to the existence of a non-zero overall piezoelectric tensor. The applied electric field 'poles' the crystals with a preferred direction of remanent polarisation. After extensive ferroelectric transformation, some of the crystal variants present become depleted, having zero volume fraction. The corresponding transformation-systems become inactive and there is a saturation in remanent strain and polarisation. Note that after loading to a high level of electric field ($E_3/E_0 = 4$) there is slight non-linearity in the D_3 versus E_3 and ε_{33} versus E_3 curves during unloading of the applied

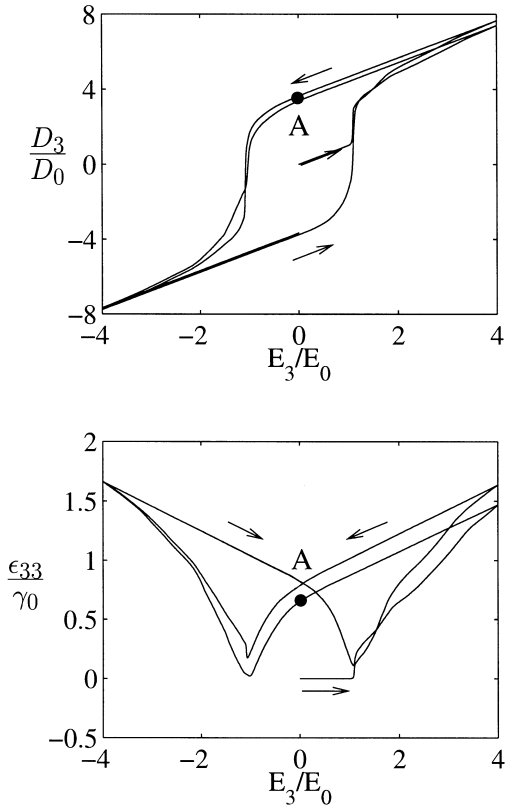

Fig. 3. Self-consistent estimates of the electrical displacement and the strain responses of a ferroelectric polycrystal to cyclic electric field loading.

field. This results from the presence of residual stresses and electric fields in the individual crystals which arise from the mismatch in strain and electric displacement between each crystal and the surrounding matrix.

Next, consider a loading path of cyclic uniaxial stress along the three-direction, starting in the compressive direction and with the same initial conditions as given above. The resulting uniaxial stress σ_{33} versus strain ε_{33} loops are given in Fig. 4. Switching initiates at $\sigma_{33}/\tau_0 = -2$ and $\varepsilon_{33}/\gamma_0 = -1/(1+\nu)$ and the progression of remanent straining followed by lock-up is evident as the hysteresis loop is traversed. Note that the hysteresis loops for transverse strains ε_{11} and ε_{22} are identical, indicating that axial symmetry is preserved. This feature was not forced by the modelling procedure, but arises through the hardening of transformation systems which are active simultaneously. During loading with stress component σ_{33} from an initially unpolarised state, the electric displacement D_i and the piezoelectric tensor d_{ikl} remain at zero throughout.

It is well-known that the application of stress can depolarise a previously poled ferroelectric. We illustrate this phenomenon by first polarising the tetragonal polycrystal to a state A by applying and then removing an electric field of strength $E_3/E_0 = 4$, as shown in Fig. 3. At this stage, the polycrystal is poled with a remanent polarisation $D_3/D_0 = 3.7$ and a remanent strain $\varepsilon_{33}/\gamma_0 = 0.8$. A compressive stress σ_{33} of magnitude $8\tau_0$ is then applied to the poled polycrystal and the resulting changes in polarisation D_3/D_0 and strain $\varepsilon_{33}/\gamma_0$ are given in Fig. 5. Finally, on unloading the stress to zero (state B in Fig. 5), the remanent polarisation is reduced by about 75% to a value of $D_3/D_0 = 0.95$. The polycrystal piezoelectric coefficient $d_{333} \equiv \partial D_3/\partial\sigma_{33}$ is also significantly reduced by the compressive half-cycle.

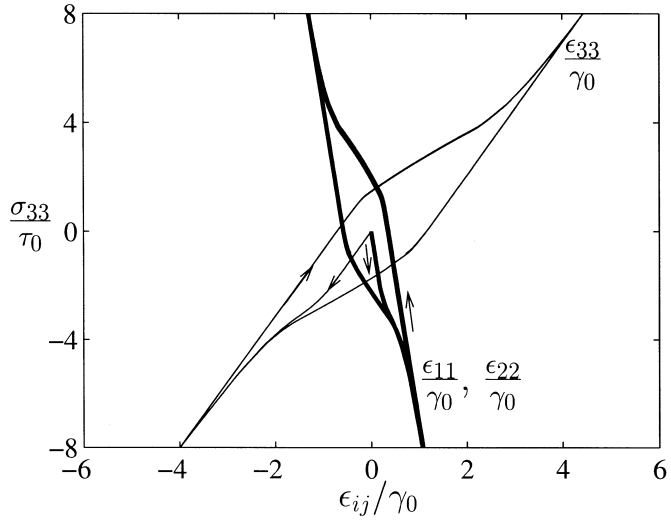

Fig. 4. Self-consistent estimates of the strain response of a ferroelectric polycrystal to cyclic uniaxial stress.

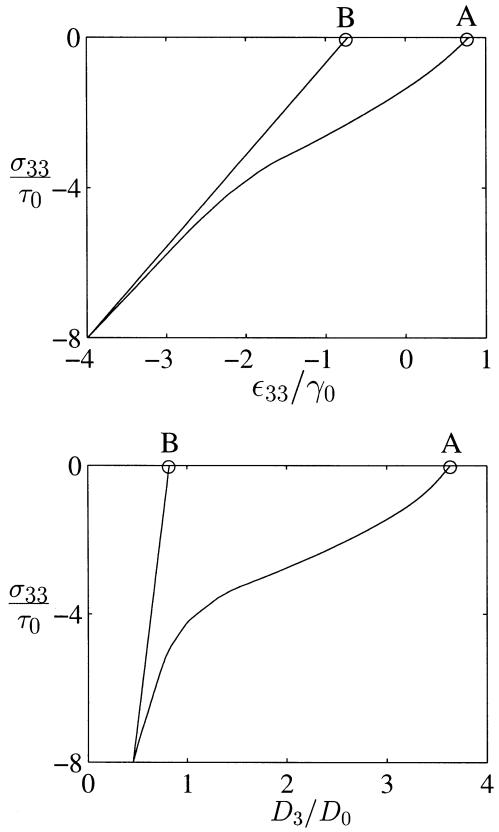

Fig. 5. Self-consistent estimates of the electrical displacement and the strain responses of a ferroelectric polycrystal to compressive stress, after previous poling by an electric field. The state A is the initial, poled state and corresponds to the point A in Fig. 3. The state B is the final state, after depoling by the compressive stress σ_{33}.

5.1. *Initial switching* (*yield*) *surfaces in electric field space and stress space*

The switching surface for a ferroelectric polycrystal may be defined as the surface in loading space (σ_{ij}, E_i) enclosing loading points at which no ferroelectric transformations occur. Provided one point within the switching surface is known, points on the switching surface may be found using a series of proportional loading excursions from the known point within the switching surface, up to the point at which a transformation system first becomes active.

Consider first the ferroelectric polycrystal specified above, in the initial, isotropic state, subjected to a series of loading operations with electric field E_3, entering the non-linear regime. After each loading operation, the polycrystal is unloaded to $E_3 = 0$ and the switching surface is determined. This loading path is shown in Fig. 6, with points A, B, C and D corresponding to the initial state and to the unloaded states

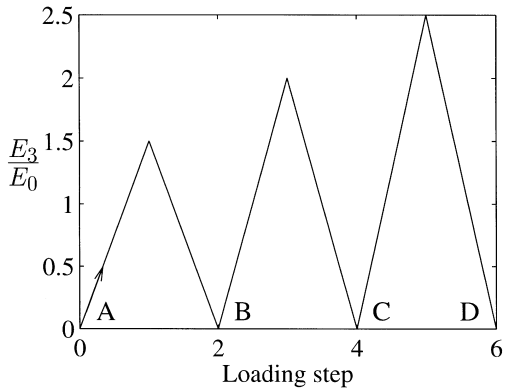

Fig. 6. Electric field loading path for polycrystal from the initial state. Points A, B, C and D correspond to unloaded states.

after loading operations up to $E_3/E_0 = 1.5$, 2.0 and 2.5, respectively. The self-consistent estimate of the dielectric response is shown in Fig. 7. After increasingly severe electric field loading, increasing levels of remanent polarisation are generated upon unloading. In order to explore the switching surface in stress–electric field space, we consider two sections;

—the switching surface in (E_3, E_1) space, with the component E_2 and the stress held at zero, as shown in Fig. 8(a) and
—the switching surface in axisymmetric stress space $(\sigma_{33}, \sigma_{11} = \sigma_{22})$, with vanishing electric field, as shown in Fig. 8(b).

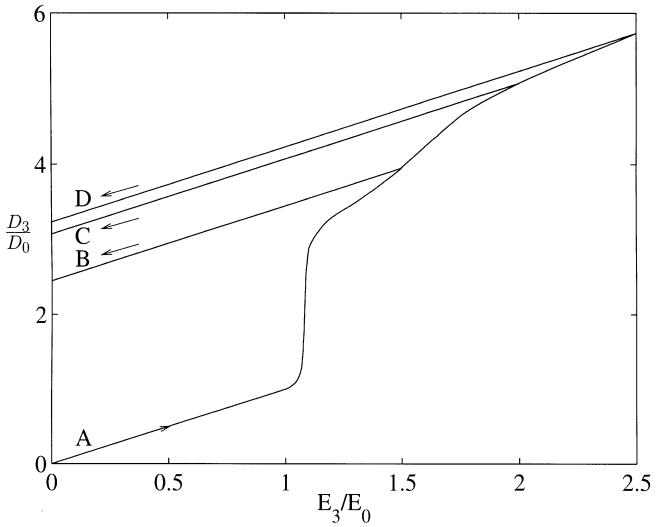

Fig. 7. Self-consistent estimates of the electrical displacement response to the loading path given in Fig. 6.

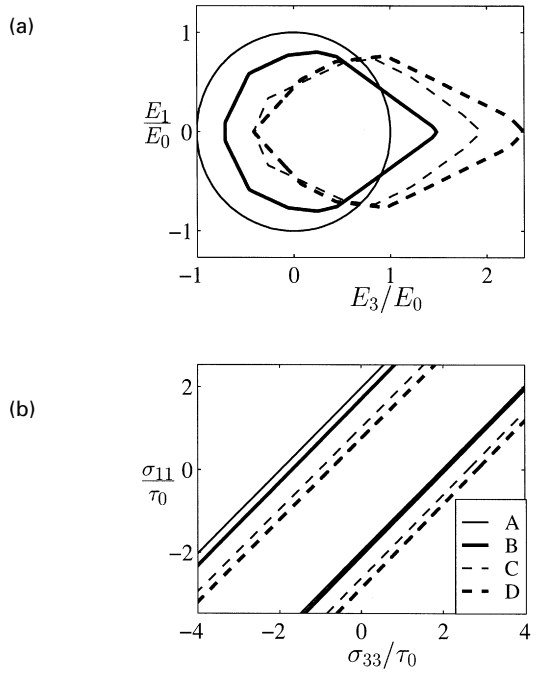

Fig. 8. Self-consistent estimates of the switching surface in states A–D, after the electric field loading shown in Fig. 6: (a) slice through the switching surface in (E_3, E_1) space, with the component E_2 and the stress held at zero; and (b) slice through the switching surface in axisymmetric stress space $(\sigma_{33}, \sigma_{11} = \sigma_{22})$, with vanishing electric field.

In the initial state A, the polycrystal is isotropic and has a circular switching surface in (E_3, E_1) space, see Fig. 8(a). Loading into the non-linear regime results in the development of a cornered switching surface, which remains upon unloading to states B, C and D, again see Fig. 8(a). An electrical analogue of the Bauschinger effect is evident: the magnitude of the electric field E_3 to cause reversed ferroelectric transformation is reduced by previous transformation in the forward direction. Next, consider the switching surface in stress space $(\sigma_{33}, \sigma_{11} = \sigma_{22})$ with a vanishing electric field, as sketched in Fig. 8(b) for the states A–D. The switching surface sections appear as pairs of straight lines since the transformation systems are insensitive to hydrostatic stresses. The effect of prior transformation by electric field loading along the three-direction is to increase the switching strength along the σ_{33}-axis slightly and to reduce the switching strength along the σ_{11}-axis. The development of a corner on the switching (i.e. yield) surface at the loading point is well-known and is expected from basic micromechanical considerations of polycrystals, as discussed by Hill (1967) and as illustrated by Hutchinson (1970) for elastic–plastic polycrystals. Such corner development leads to a drop in the instantaneous moduli compared with that for a smooth switching surface and to the greater likelihood of material instabilities.

We complete this section by calculating the evolution of the switching surface from

the initial, isotropic state, due to loading into the non-linear range by a compressive stress σ_{33}. Figure 9 shows the predicted response of the polycrystal after the loading operations $\sigma_{33}/\tau_0 = -3, -4, -5$, in each case followed by unloading. The points A′, B′, C′ and D′ correspond to the unloaded states after each loading operation. Slices through the switching surface are shown in Fig. 10, as follows. In Fig. 10(a) the switching surface is probed with the electric field components (E_3, E_1) and $E_2 = \sigma_{ij} = 0$. In Fig. 10(b), the electric field is held at zero and axisymmetric stresses $(\sigma_{33}, \sigma_{11} = \sigma_{22})$ are applied. We note that uniaxial stressing into the non-linear range has the effect of shrinking the switching surface in (E_3, E_1) space, Fig. 10(a). The switching surface in $(\sigma_{33}, \sigma_{11} = \sigma_{22})$ space is translated such that compressive strength in the three-direction increases and in the one-direction decreases due to prior remanent straining along the three-direction.

6. Concluding remarks

The self-consistent crystal plasticity scheme of Hill (1965a, b) and Hutchinson (1970) has been extended to address the case of ferroelectric switching. The self-consistent scheme uses a single crystal constitutive law for the ferroelectric, which extends the framework of crystal plasticity theory. An analogy is drawn between the slip systems of dislocation plasticity in metals and transformation plasticity by domain wall movement in ferroelectrics. It allows for changes in the linear properties of a crystal and for the 'lock-up' phenomenon caused by complete transformation. The micromechanical scheme is based on an abstraction of structures observed in real ferroelectric materials and with the exception of a small hardening rate, all aspects of

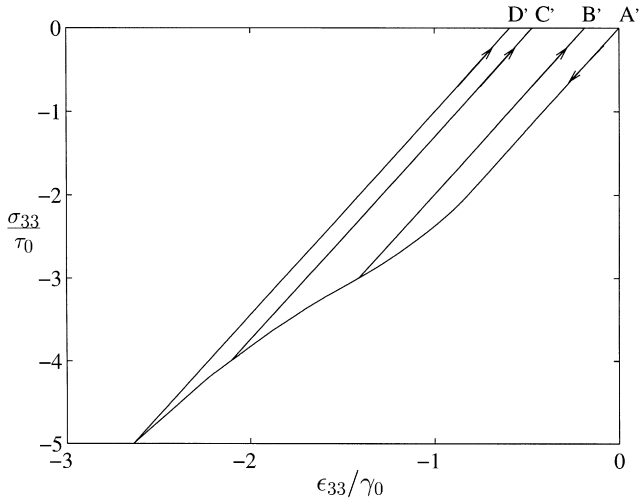

Fig. 9. Self-consistent estimates of the strain response to various levels of uniaxial compression. Points A′, B′, C′ and D′ correspond to unloaded states.

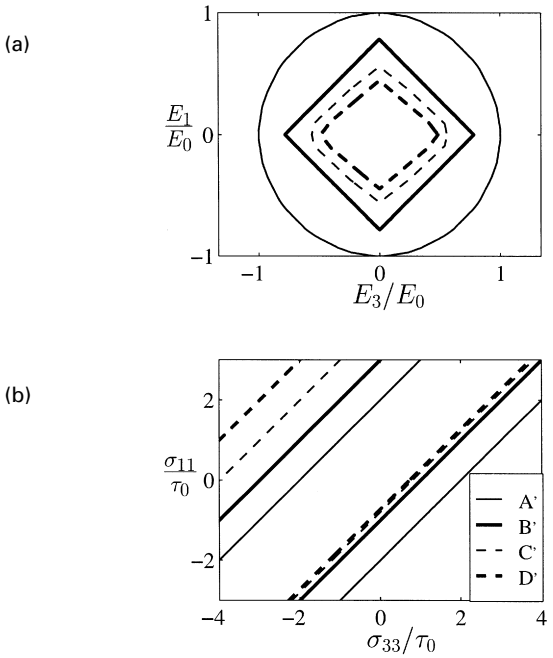

Fig. 10. Self-consistent estimates of the switching surface in states A′–D′, after uniaxial compression shown in Fig. 9: (a) slice through the switching surface in (E_3, E_1) space, with the component E_2 and the stress held at zero; and (b) slice through the switching surface in axisymmetric stress space ($\sigma_{33}, \sigma_{11} = \sigma_{22}$), with vanishing electric field.

the model are justifiable on physical grounds. A positive hardening rate is required to stabilise the numerical scheme, but this can be small enough to make a negligible difference to the simulated behavior of the crystal.

The self-consistent scheme allows the response of a polycrystal to various types of loading to be simulated. An essential ingredient is the self-consistent determination of the tangent moduli for the non-linear ferroelectric during switching. It has been necessary to obtain expressions for the constraint imposed on an ellipsoidal piezoelectric inclusion by a piezoelectric matrix. The self-consistent model captures in a qualitative way several observed features of ferroelectrics which have been reported in the literature. These include the smooth shapes of the dielectric hysteresis and butterfly hysteresis loops, a polycrystal Bauschinger effect in both mechanical and electrical loading and the depolarisation of a polycrystal by compressive stresses. Initial switching surfaces in plane stress space and in electric field space have been presented. They are found to be convex and show corners where non-linear deformation has occurred. Several subtle features of the behaviour of the model are illustrated in these switching surfaces, including the way in which pre-loading with electric field modifies the critical stresses required to induce switching in compression and tension in directions parallel to and perpendicular to the electric field. These results are relevant to the design of ferroelectric devices, where a single overload of

stress may severely affect performance. The polycrystal model allows the response of a ferroelectric material to any loading path to be estimated.

Acknowledgements

The work of C.M.L. and R.M.M. was supported by Grant 9813022 from the National Science Foundation. J.E.H. acknowledges support from the E.P.S.R.C.

Appendix A: Eshelby tensors and constraint tensors for a piezoelectric solid

In this Appendix, expressions for the piezoelectric Eshelby tensors are derived. The numerical procedure for construction of the Eshelby tensors follows that outlined by Ghahremani (1977) for an ellipsoidal inclusion in an anisotropic elastic solid. The development has some similarity to that given by Dunn (1994), but the Eshelby tensors given here are for the transformation problem expressed in terms of strain and the electric displacement and not the strain and electric field as given by Dunn (1994). The derivation given here follows closely that used by Eshelby, in which an inclusion is (i) removed from the matrix and allowed to transform, (ii) returned to its original shape by surface tractions and put back in its matrix and (iii) released.

Consider an infinite linear piezoelectric medium containing an ellipsoidal inclusion with surface specified by

$$\left(\frac{x_1}{a}\right)^2+\left(\frac{x_2}{b}\right)^2+\left(\frac{x_3}{c}\right)^2=1 \tag{A.1}$$

where the Cartesian axes x_i are aligned with the principal axes of the ellipsoid, of length (a,b,c). Assume that the inclusion undergoes a stress-free transformation strain and an electric field-free polarisation, $(\varepsilon_{ij}^T, D_i^T)$. For example, the transformation strain can be due to plastic strain in the inclusion and the transformation polarisation due to remanency. It is assumed that the matrix does not transform and that the stress and electric field vanish at infinity. Let the final constrained state of strain and polarisation in the inclusion embedded in the matrix be denoted by $(\varepsilon_{ij}^c, D_i^c)$. Then, the problem is to evaluate the Eshelby tensors $S_{ijkl}^{\varepsilon\varepsilon}$, $S_{kij}^{\varepsilon D}$, $S_{ikl}^{D\varepsilon}$, S_{ik}^{DD} where

$$\begin{pmatrix}\varepsilon_{ij}^c\\ D_i^c\end{pmatrix}=\begin{bmatrix}S_{ijkl}^{\varepsilon\varepsilon} & S_{kij}^{\varepsilon D}\\ S_{ikl}^{D\varepsilon} & S_{ik}^{DD}\end{bmatrix}\begin{pmatrix}\varepsilon_{kl}^T\\ D_k^T\end{pmatrix} \tag{A.2}$$

Following Eshelby (1957), the final constrained state of strain and electric displacement in the transformed inclusion is found by linear superposition of the effects

of a set of body forces and point charges on the surface of the inclusion. It is convenient to divide the problem up into a series of steps as sketched in Fig. A1 and given below.

Step (*i*). Remove the inclusion from the matrix and place it in a medium with properties $c^D_{ijkl} = 0$, $h_{kij} = 0$ and $\beta^{\varepsilon}_{ij} = 0$. Allow the inclusion to transform to a strain ε^T_{ij} and an electric displacement D^T_i with vanishing stress and electric field. In the medium surrounding the inclusion, the stress and electric field vanish and the strain equals ε^T_{ij}. By applying an appropriate distribution of point charge $Q' = -D^T_i n_i$ on the surface of the inclusion (with unit outward normal n_i) the electric displacement also vanishes in the surrounding medium.

Step (*ii*). Restore the inclusion to a state of vanishing strain and electric field, $\varepsilon_{ij} = 0$ and $E_i = 0$, by imposing an appropriate value of stress $-\sigma^p_{ij}$ and electric displacement $-D^p_i$ in the inclusion. The elastic piezoelectric constitutive law demands that

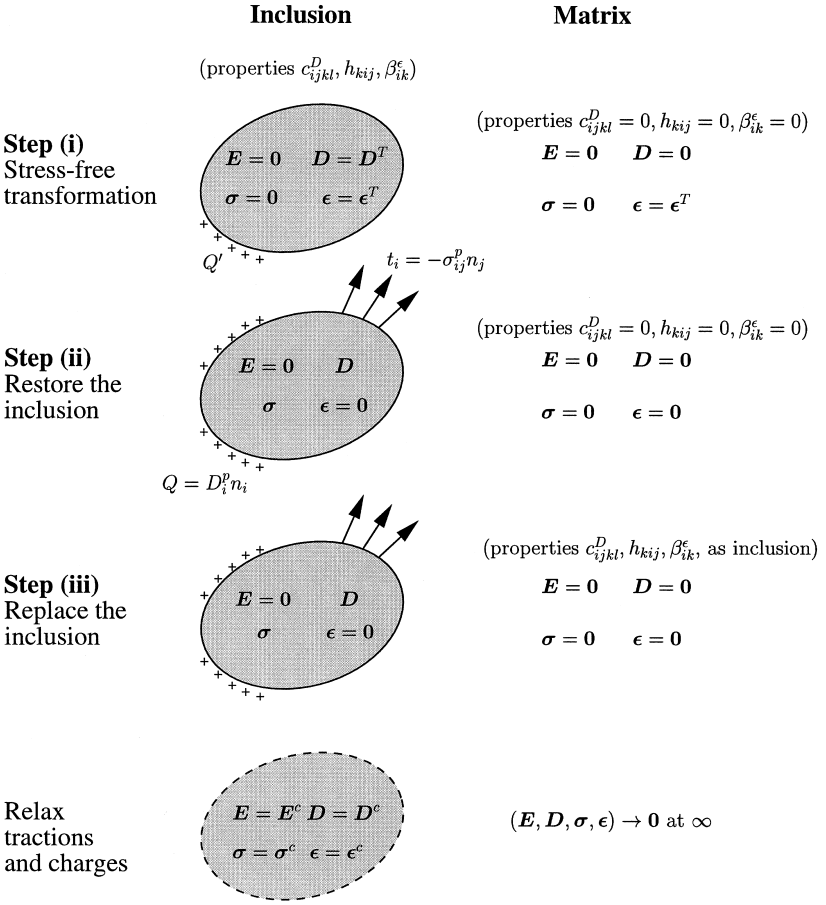

Fig. A1. Steps in calculating Eshelby tensors for a piezoelectric solid.

$$-\sigma_{ij}^{p} = c_{ijkl}^{E}(\varepsilon_{kl}-\varepsilon_{kl}^{T})-e_{kij}E_{k} \tag{A.3a}$$

and

$$-D_{i}^{p}-D_{i}^{T} = e_{ikl}(\varepsilon_{kl}-\varepsilon_{kl}^{T})+\kappa_{ik}^{\varepsilon}E_{k} \tag{A.3b}$$

giving here,

$$\sigma_{ij}^{p} = c_{ijkl}^{E}\varepsilon_{kl}^{T} \tag{A.4a}$$

and

$$D_{i}^{p} = -D_{i}^{T}+e_{ikl}\varepsilon_{kl}^{T} \tag{A.4b}$$

The required state $(-\sigma_{ij}^{p}, -D_{i}^{p})$ within the inclusion is attained by applying surface tractions

$$t_{i} = -\sigma_{ij}^{p}n_{j} \tag{A.5a}$$

and a net surface charge distribution

$$Q = D_{i}^{p}n_{i} \tag{A.5b}$$

on the surface of the inclusion, with $\boldsymbol{n}$ still defined as the unit outward normal at the surface of the inclusion. In the matrix, the stress, strain, electric field and electric displacement all vanish and the piezoelectric moduli are recovered to equal their non-zero values.

Step (*iii*). The inclusion is put back into the infinite matrix and body forces $f_{i} = \sigma_{ij}^{p}n_{j}$ and body charges $q = -D_{i}^{p}n_{i}$ are applied over the surface of the inclusion in the infinite solid in order to cancel the surface traction and surface charge of step (ii). The inclusion is thereby released back into its cavity. The resulting constrained values of the displacement field $u_{i}(x_{j})$ and the electric potential $\Phi(x_{j})$ at any point within the inclusion or matrix are obtained in terms of the Green's functions $(G_{ij}^{uf}(\boldsymbol{x}-\boldsymbol{x}'), G_{j}^{\Phi f}(\boldsymbol{x}-\boldsymbol{x}'), G_{i}^{uq}(\boldsymbol{x}-\boldsymbol{x}'), G^{\Phi q}(\boldsymbol{x}-\boldsymbol{x}'))$, as summarised in Appendix B. The result is simply quoted here

$$u_{i}(\boldsymbol{x}) = \int_{S'}[G_{ij}^{uf}(\boldsymbol{x}-\boldsymbol{x}')f_{j}(\boldsymbol{x}')]\,\mathrm{d}S' + \int_{S'}[G_{i}^{uq}(\boldsymbol{x}-\boldsymbol{x}')q(\boldsymbol{x}')]\,\mathrm{d}S' \tag{A.5a}$$

and

$$\Phi(\boldsymbol{x}) = \int_{S'}[G_{j}^{\Phi f}(\boldsymbol{x}-\boldsymbol{x}')f_{j}(\boldsymbol{x}')]\,\mathrm{d}S' + \int_{S'}[G^{\Phi q}(\boldsymbol{x}-\boldsymbol{x}')q(\boldsymbol{x}')]\,\mathrm{d}S' \tag{A.5b}$$

where $f_{i} = \sigma_{ij}^{p}n_{j}$ and $q = -D_{i}^{p}n_{i}$. We can interpret the Green's function $G_{ij}^{uf}(\boldsymbol{x}-\boldsymbol{x}')$ as the displacement in the i-direction at an arbitrary point $\boldsymbol{x}$ and $G_{j}^{\Phi f}(\boldsymbol{x}-\boldsymbol{x}')$ as the associated electric potential, due to a unit point load in the j-direction at $\boldsymbol{x}'$. Similarly, $G_{i}^{uq}(\boldsymbol{x}-\boldsymbol{x}')$ is the displacement in the i-direction and $G^{\Phi q}(\boldsymbol{x}-\boldsymbol{x}')$ is the electric potential, both due to a unit point charge at $\boldsymbol{x}'$.

The constrained displacement field and potential throughout the solid can be rewritten from (A.5) as

$$u_i(\boldsymbol{x}) = \sigma^p_{jk} \int_{S'} [G^{uf}_{ij}(\boldsymbol{x}-\boldsymbol{x}')n_k(\boldsymbol{x}')]\,\mathrm{d}S' - D^p_k \int_{S'} [G^{uq}_{i}(\boldsymbol{x}-\boldsymbol{x}')n_k(\boldsymbol{x}')]\,\mathrm{d}S' \tag{A.6a}$$

and

$$\Phi(\boldsymbol{x}) = \sigma^p_{jk} \int_{S'} [G^{\Phi f}_{j}(\boldsymbol{x}-\boldsymbol{x}')n_k(\boldsymbol{x}')]\,\mathrm{d}S' - D^p_k \int_{S'} [G^{\Phi q}(\boldsymbol{x}-\boldsymbol{x}')n_k(\boldsymbol{x}')]\,\mathrm{d}S' \tag{A6.b}$$

Application of the divergence theorem to (A.6a,b) and use of the definitions (2.2) and (2.8), generates expressions for the constrained strain ε^c_{ij} and electric field E^c_i in the inclusion

$$\begin{pmatrix} \varepsilon^c_{ij} \\ E^c_i \end{pmatrix} = \begin{bmatrix} P^{uf}_{ijpq} & P^{uq}_{qij} \\ P^{\Phi f}_{ipq} & P^{\Phi q}_{iq} \end{bmatrix} \begin{pmatrix} \sigma^p_{pq} \\ D^p_q \end{pmatrix} \tag{A.7}$$

where

$$P^{uf}_{ijpq} = -\int_{V'} \left[\frac{\partial^2 G^{uf}_{ip}(\boldsymbol{x}-\boldsymbol{x}')}{\partial x_j\, \partial x_q} \right]_{(i,j)(p,q)} \mathrm{d}V' \tag{A.8a}$$

$$P^{uq}_{qij} = \int_{V'} \left[\frac{\partial^2 G^{uq}_{i}(\boldsymbol{x}-\boldsymbol{x}')}{\partial x_j\, \partial x_q} \right]_{(i,j)} \mathrm{d}V' \tag{A.8b}$$

$$P^{\Phi f}_{ipq} = \int_{V'} \left[\frac{\partial^2 G^{\Phi f}_{p}(\boldsymbol{x}-\boldsymbol{x}')}{\partial x_i\, \partial x_q} \right]_{(p,q)} \mathrm{d}V' \tag{A.8c}$$

$$P^{\Phi q}_{iq} = -\int_{V'} \left[\frac{\partial^2 G^{\Phi q}(\boldsymbol{x}-\boldsymbol{x}')}{\partial x_i\, \partial x_q} \right] \mathrm{d}V' \tag{A.8d}$$

where the subscript label (i,j) denotes symmetrisation with respect to i and j and so on. Note that the Green's function and the associated P-tensors must be interpreted as generalised functions, with the above statements as formal definitions. A numerical scheme is outlined in Appendix B for evaluation of the P-tensors. In the remainder of this Appendix, we derive the Eshelby S-tensors (A.2) in terms of the P-tensors and then we construct the constraint tensors relating to the uniform stress and electric field within an ellipsoidal cavity to the uniform strain and electric displacement.

Construction of the Eshelby S-tensors and constraint tensors for the ellipsoidal cavity

The Eshelby S-tensors, as defined by (A.2) are determined by expressing (σ^p_{ij}, D^p_i) in terms of (σ^T_{ij}, D^T_i), upon making use of (2.5b), written in the form

$$D_i^c - D_i^T = e_{ijk}(\varepsilon_{jk}^c - \varepsilon_{jk}^T) + \kappa_{ij}^{\varepsilon} E_j^c \tag{A.9}$$

The result is

$$S_{ijkl}^{\varepsilon\varepsilon} \equiv P_{ijpq}^{uf} c_{pqkl}^E + P_{qij}^{uq} e_{qkl} \tag{A.10a}$$

$$S_{qij}^{\varepsilon D} \equiv -P_{qij}^{uq} \tag{A.10b}$$

$$S_{imn}^{D\varepsilon} \equiv e_{ijk} S_{jkmn}^{\varepsilon\varepsilon} - e_{imn} + \kappa_{it}^{\varepsilon} P_{tpq}^{\Phi f} c_{pqmn}^E + \kappa_{it}^{\varepsilon} P_{tq}^{\Phi q} e_{qmn} \tag{A.10c}$$

$$S_{it}^{DD} \equiv \delta_{it} + e_{ijk} S_{tjk}^{\varepsilon D} - \kappa_{iq}^{\varepsilon} P_{qt}^{\Phi q} \tag{A.10d}$$

Following the prescription of Hill (1965a, b), constraint tensors for the inclusion are defined by considering an anisotropic piezoelectric matrix containing an ellipsoidal void with the same orientation and shape as the inclusion. The boundary of the cavity is subjected to a traction $\sigma_{ij}^* n_j$ and a potential $\Phi = -E_i^* x_i$, where σ_{ij}^* and E_i^* are uniform. The associated uniform strain ε_{ij}^* and electric displacement D_i^* in the void is related to (σ_{ij}^*, E_i^*) by a constraint tensor according to

$$\begin{pmatrix} \sigma_{ij}^* \\ E_i^* \end{pmatrix} = -\begin{bmatrix} c_{ijkl}^{D^*} & -h_{kij}^* \\ -h_{ikl}^* & \beta_{ik}^{\varepsilon^*} \end{bmatrix} \begin{pmatrix} \varepsilon_{kl}^* \\ D_k^* \end{pmatrix} \tag{A.11}$$

Specific expressions for the constraint tensor are obtained as follows. Consider again the transformation of an inclusion in an infinite matrix of identical elastic properties. The constrained strain ε_{kl}^* and electrical displacement D_k^* after transformation is related to the stress-free transformation strain by (A.2). The stress and electric field remote from the inclusion vanish and the final stress and electric field within the transformed inclusion are given by

$$\sigma_{ij}^* = c_{ijkl}^D(\varepsilon_{kl}^* - \varepsilon_{kl}^T) - h_{kij}(D_k^* - D_k^T) \tag{A.12a}$$

and

$$E_i^* = -h_{ikl}(\varepsilon_{kl}^* - \varepsilon_{kl}^T) + \beta_{ik}^{\varepsilon}(D_k^* - D_k^T) \tag{A.12b}$$

Now invert (A.2) in order to express $(\varepsilon_{ij}^T, D_i^T)$ in terms of $(\varepsilon_{ij}^*, D_i^*)$ and write

$$\begin{pmatrix} \varepsilon_{ij}^T \\ D_i^T \end{pmatrix} = \begin{bmatrix} T_{ijkl}^{\varepsilon\varepsilon} & T_{kij}^{\varepsilon D} \\ T_{ikl}^{D\varepsilon} & T_{ik}^{DD} \end{bmatrix} \begin{pmatrix} \varepsilon_{kl}^* \\ D_k^* \end{pmatrix} \tag{A.13}$$

where the T-tensors are the inversion of the S-tensor of (A.2). Substitution of (A.13) into (A.12a,b) and identification of the result with (A.11) provides the desired explicit expressions for the constraint tensors.

$$c_{ijkl}^{D^*} = -c_{ijkl}^D + c_{ijpq}^D T_{pqkl}^{\varepsilon\varepsilon} - h_{pij} T_{pkl}^{D\varepsilon} \tag{A.14a}$$

$$h_{kij}^* = -h_{kij} - c_{ijpq}^D T_{kpq}^{\varepsilon D} + h_{pij} T_{pk}^{DD}$$

$$= -h_{kij} + h_{kpq} T^{\varepsilon\varepsilon}_{pqij} - \beta^{\varepsilon}_{kp} T^{D\varepsilon}_{pij} \tag{A.14b}$$

and

$$\beta^{\varepsilon^*}_{ik} = -\beta^{\varepsilon}_{ik} - h_{ipq} T^{\varepsilon D}_{kpq} + \beta^{\varepsilon}_{ip} T^{DD}_{pk} \tag{A.14c}$$

Appendix B: Numerical scheme for evaluation of the P-tensors

A numerical scheme is outlined here to evaluate the P-tensors, as defined in (A.8). The approach expands upon that of Ghahremani (1977) for an ellipsoidal inclusion in an anisotropic elastic solid and gives rise to a two-dimensional integral over the unit sphere, in preference to the algebraically more complex one-dimensional integral over the unit circle from a Radon transform as developed by Willis (1965).

As the starting point, consider the governing partial differential equations for the displacement and the electric potential for a linear piezoelectric solid of constitutive law

$$\sigma_{ij} = c^{E}_{ijkl} \varepsilon_{kl} - e_{kij} E_k \tag{B.1a}$$

and

$$D_i = e_{ikl} \varepsilon_{kl} + \kappa^{\varepsilon}_{ik} E_k \tag{B1.b}$$

Upon making use of (2.6)–(2.8) and upon introducing the forward operator $\partial_i \equiv \partial/\partial x_i$ we have

$$\begin{bmatrix} c^{E}_{ijkl}\,\partial_l\,\partial_j & e_{kij}\,\partial_k\,\partial_j \\ e_{jki}\,\partial_i\,\partial_j & -\kappa^{\varepsilon}_{ij}\,\partial_i\,\partial_j \end{bmatrix} \begin{pmatrix} u_k \\ \Phi \end{pmatrix} + \begin{pmatrix} f_i \\ -q \end{pmatrix} = 0 \tag{B.2}$$

with vanishing (u_i, Φ) at infinity. Our strategy is to solve for (u_i, Φ), for a given distribution of body force $f_i = \sigma^{p}_{ij} n_j$ and $q = -D^{p}_{i} n_i$ on the surface of an ellipsoidal inclusion of unit outward normal $\boldsymbol{n}$, for the case where the piezoelectric properties of the inclusion equal those of the medium. Formulae for $(\sigma^{p}_{ij}, D^{p}_{i})$ have already been specified by (A.4).

The Green's function associated with (B.2) satisfies the self-adjoint equations

$$\begin{bmatrix} c^{E}_{ijkl}\,\partial_l\,\partial_j & e_{kij}\,\partial_k\,\partial_j \\ e_{jki}\,\partial_i\,\partial_j & -\kappa^{\varepsilon}_{ij}\,\partial_i\,\partial_j \end{bmatrix} \begin{bmatrix} G^{uf}_{kp}(\boldsymbol{x}-\boldsymbol{x}') & G^{\Phi f}_{k}(\boldsymbol{x}-\boldsymbol{x}') \\ G^{uq}_{p}(\boldsymbol{x}-\boldsymbol{x}') & G^{\Phi q}(\boldsymbol{x}-\boldsymbol{x}') \end{bmatrix} + \begin{bmatrix} \delta_{ip}\delta(\boldsymbol{x}-\boldsymbol{x}') & 0 \\ 0 & -\delta(\boldsymbol{x}-\boldsymbol{x}') \end{bmatrix} = 0 \tag{B.3}$$

with the Green's functions vanishing at infinity. Linear superposition gives

$$u_i(\boldsymbol{x}) = \int_{V'} [G_{ip}^{uf}(\boldsymbol{x}-\boldsymbol{x}')f_p(\boldsymbol{x}') + G_i^{uq}(\boldsymbol{x}-\boldsymbol{x}')q(\boldsymbol{x}')]\,\mathrm{d}V' \tag{B.4a}$$

and

$$\Phi(\boldsymbol{x}) = \int_{V'} [G_i^{\Phi f}(\boldsymbol{x}-\boldsymbol{x}')f_i(\boldsymbol{x}') + G^{\Phi q}(\boldsymbol{x}-\boldsymbol{x}')q(\boldsymbol{x}')]\,\mathrm{d}V' \tag{B.4b}$$

as the desired solution. In the Eshelby inclusion problem (step (iii) detailed in Appendix A), we seek the displacement and electric potential due to a distribution of surface forces $f_i = \sigma_{ij}^p n_j$ and surface charges $q = -D_i^p n_i$ on the surface of the ellipsoidal inclusion. Consequently, the volume integrals of (B.4a,b) are replaced by surface integrals over the inclusion, as given in (A.5a,b) and (A.6a,b). The uniform strain and electric field within the inclusion follows as (A.7), with the P-tensors expressed in terms of derivatives of the Green's function via (A.8). These expressions for the P-tensors are evaluated numerically by taking the Fourier transforms of the Green's functions as follows.

For a later reduction, we change variables from x_i to the scaled coordinates

$$x_1 \to \bar{x}_1 \equiv x_1/a \quad x_2 \to \bar{x}_2 \equiv x_2/b \quad x_3 \to \bar{x}_3 \equiv x_3/c \tag{B.5}$$

Now let $\bar{G}_{ip}^{uf}(\bar{\boldsymbol{x}}) = G_{ip}^{uf}(\boldsymbol{x})$ and define $\hat{G}_{ip}^{uf}(\boldsymbol{k})$ as the three-dimensional Fourier transform of $\bar{G}_{ip}^{uf}(\bar{\boldsymbol{x}})$, so that

$$\hat{G}_{ip}^{uf}(\boldsymbol{k}) \equiv \int_{-\infty}^{\infty} [\mathrm{e}^{-i\boldsymbol{k}\cdot\bar{\boldsymbol{x}}}\bar{G}_{ip}^{uf}(\bar{\boldsymbol{x}})]\,\mathrm{d}\bar{V} \Leftrightarrow \bar{G}_{ip}^{uf}(\bar{\boldsymbol{x}}) \equiv \frac{1}{8\pi^3}\int_{-\infty}^{\infty} [\mathrm{e}^{i\boldsymbol{k}\cdot\bar{\boldsymbol{x}}}\hat{G}_{ip}^{uf}(\boldsymbol{k})]\,\mathrm{d}V_k \tag{B.6a}$$

In identical fashion, we take $\bar{G}_i^{\Phi f}(\bar{\boldsymbol{x}}) = G_i^{\Phi f}(\boldsymbol{x})$, $\bar{G}_i^{uq}(\bar{\boldsymbol{x}}) = G_i^{uq}(\boldsymbol{x})$ and $\bar{G}^{\Phi q}(\bar{\boldsymbol{x}}) = G^{\Phi q}(\boldsymbol{x})$ and define $(\hat{G}_i^{\Phi f}(\boldsymbol{k}), \hat{G}_i^{uq}(\boldsymbol{k}), \hat{G}^{\Phi q}(\boldsymbol{k}))$ as the three-dimensional Fourier transforms of $(\bar{G}_i^{\Phi f}(\bar{\boldsymbol{x}}), \bar{G}_i^{uq}(\bar{\boldsymbol{x}}), \bar{G}^{\Phi q}(\bar{\boldsymbol{x}}))$, respectively, giving

$$\hat{G}_i^{\Phi f}(\boldsymbol{k}) \equiv \int_{-\infty}^{\infty} [\mathrm{e}^{-i\boldsymbol{k}\cdot\bar{\boldsymbol{x}}}\bar{G}_i^{\Phi f}(\bar{\boldsymbol{x}})]\,\mathrm{d}\bar{V} \Leftrightarrow \bar{G}_i^{\Phi f}(\bar{\boldsymbol{x}}) \equiv \frac{1}{8\pi^3}\int_{-\infty}^{\infty} [\mathrm{e}^{i\boldsymbol{k}\cdot\bar{\boldsymbol{x}}}\hat{G}_i^{\Phi f}(\boldsymbol{k})]\,\mathrm{d}V_k \tag{B.6b}$$

$$\hat{G}_i^{uq}(\boldsymbol{k}) \equiv \int_{-\infty}^{\infty} [\mathrm{e}^{-i\boldsymbol{k}\cdot\bar{\boldsymbol{x}}}\bar{G}_i^{uq}(\bar{\boldsymbol{x}})]\,\mathrm{d}\bar{V} \Leftrightarrow \bar{G}_i^{uq}(\bar{\boldsymbol{x}}) \equiv \frac{1}{8\pi^3}\int_{-\infty}^{\infty} [\mathrm{e}^{i\boldsymbol{k}\cdot\bar{\boldsymbol{x}}}\hat{G}_i^{uq}(\boldsymbol{k})]\,\mathrm{d}V_k \tag{B.6c}$$

$$\hat{G}^{\Phi q}(\boldsymbol{k}) \equiv \int_{-\infty}^{\infty} [\mathrm{e}^{-i\boldsymbol{k}\cdot\bar{\boldsymbol{x}}}\bar{G}^{\Phi q}(\bar{\boldsymbol{x}})]\,\mathrm{d}\bar{V} \Leftrightarrow \bar{G}^{\Phi q}(\bar{\boldsymbol{x}}) \equiv \frac{1}{8\pi^3}\int_{-\infty}^{\infty} [\mathrm{e}^{i\boldsymbol{k}\cdot\bar{\boldsymbol{x}}}\hat{G}^{\Phi q}(\boldsymbol{k})]\,\mathrm{d}V_k \tag{B.6d}$$

Explicit formulae for the Fourier transforms of the Green's functions are obtained by taking Fourier transforms of (B.3), viz

$$(abc)\begin{bmatrix} c^E_{ijkl}Q_lQ_j & e_{kij}Q_kQ_j \\ -e_{jki}Q_iQ_j & \kappa^\varepsilon_{ij}Q_iQ_j \end{bmatrix}\begin{bmatrix} \hat{G}^{uf}_{kp} & \hat{G}^{\Phi f}_{k} \\ \hat{G}^{uq}_{p} & \hat{G}^{\Phi q} \end{bmatrix} = \begin{bmatrix} \delta_{ip} & 0 \\ 0 & 1 \end{bmatrix} \tag{B.7}$$

where

$$Q_i \equiv \Psi_{ij}k_j \quad \text{and} \quad (\Psi_{ij}) \equiv \begin{pmatrix} 1/a & 0 & 0 \\ 0 & 1/b & 0 \\ 0 & 0 & 1/c \end{pmatrix} \tag{B.8}$$

Thus, for any value of $\boldsymbol{k}$ the Fourier transforms are obtained by inversion of (B.7). Upon making use of the inversion formulae (B.6a–d) for the Fourier transforms of the Green's functions, the P-tensors defined in (A.8a–d) can be written in terms of integrals over the unit sphere $\bar{V}$ as

$$P^{uf}_{ijpq} = \frac{(abc)}{8\pi^3}\int_{\bar{V}}\frac{\mathrm{d}\bar{V}}{\bar{V}}\int_{\bar{V}'}\mathrm{d}\bar{V}'\int_{-\infty}^{\infty}\mathrm{d}V_k[\mathrm{e}^{i\boldsymbol{k}\cdot(\bar{\boldsymbol{x}}-\bar{\boldsymbol{x}}')}\hat{G}^{uf}_{ip}(\boldsymbol{k})Q_jQ_q]_{(i,j)(p,q)} \tag{B.9a}$$

$$P^{uq}_{qij} = \frac{-(abc)}{8\pi^3}\int_{\bar{V}}\frac{\mathrm{d}\bar{V}}{\bar{V}}\int_{\bar{V}'}\mathrm{d}\bar{V}'\int_{-\infty}^{\infty}\mathrm{d}V_k[\mathrm{e}^{i\boldsymbol{k}\cdot(\bar{\boldsymbol{x}}-\bar{\boldsymbol{x}}')}\hat{G}^{uq}_{i}(\boldsymbol{k})Q_jQ_q]_{(i,j)} \tag{B.9b}$$

$$P^{\Phi f}_{ipq} = \frac{-(abc)}{8\pi^3}\int_{\bar{V}}\frac{\mathrm{d}\bar{V}}{\bar{V}}\int_{\bar{V}'}\mathrm{d}\bar{V}'\int_{-\infty}^{\infty}\mathrm{d}V_k[\mathrm{e}^{i\boldsymbol{k}\cdot(\bar{\boldsymbol{x}}-\bar{\boldsymbol{x}}')}\hat{G}^{\Phi f}_{p}(\boldsymbol{k})Q_iQ_q]_{(p,q)} \tag{B.9c}$$

and

$$P^{\Phi q}_{iq} = \frac{(abc)}{8\pi^3}\int_{\bar{V}}\frac{\mathrm{d}\bar{V}}{\bar{V}}\int_{\bar{V}'}\mathrm{d}\bar{V}'\int_{-\infty}^{\infty}\mathrm{d}V_k[\mathrm{e}^{i\boldsymbol{k}\cdot(\bar{\boldsymbol{x}}-\bar{\boldsymbol{x}}')}\hat{G}^{\Phi q}(\boldsymbol{k})Q_iQ_q] \tag{B.9d}$$

The above integrals simplify considerably, upon noting that the integrands are homogeneous and of degree zero in $\boldsymbol{k}$ and so depend only upon the direction of $\boldsymbol{k}$. We introduce the spherical coordinate system (k,θ,ϕ), write $\mathrm{d}V_k = k^2\sin\theta\,\mathrm{d}k\,\mathrm{d}\theta\,\mathrm{d}\phi$ and recall the identity

$$\int_0^{\infty}\mathrm{d}k k^2\int_{\bar{V}}\frac{\mathrm{d}\bar{V}}{\bar{V}}\int_{\bar{V}'}\mathrm{d}\bar{V}'\,\mathrm{e}^{i\boldsymbol{k}\cdot(\bar{\boldsymbol{x}}-\bar{\boldsymbol{x}}')} = 2\pi^2 \tag{B.10}$$

Thence, (B.9a–d) reduce to

$$P^{uf}_{ijpq} = \frac{(abc)}{4\pi}\int_0^{\pi}\mathrm{d}\theta\sin\theta\int_0^{2\pi}\mathrm{d}\phi[\hat{G}^{uf}_{ip}(\boldsymbol{k})Q_jQ_q]_{(i,j)(p,q)} \tag{B.11a}$$

$$P^{uq}_{qij} = \frac{-(abc)}{4\pi}\int_0^{\pi}\mathrm{d}\theta\sin\theta\int_0^{2\pi}\mathrm{d}\phi[\hat{G}^{uq}_{i}(\boldsymbol{k})Q_jQ_q]_{(i,j)} \tag{B.11b}$$

$$P^{\Phi f}_{ipq} = \frac{-(abc)}{4\pi}\int_0^{\pi}\mathrm{d}\theta\sin\theta\int_0^{2\pi}\mathrm{d}\phi[\hat{G}^{\Phi f}_{p}(\boldsymbol{k})Q_iQ_q]_{(p,q)} \tag{B.11c}$$

$$P_{iq}^{\Phi q} = \frac{(abc)}{4\pi} \int_0^{\pi} \mathrm{d}\theta \sin\theta \int_0^{2\pi} \mathrm{d}\phi [\hat{G}^{\Phi q}(\boldsymbol{k}) Q_i Q_q] \tag{B.11d}$$

These integrals are evaluated by Gaussian quadrature along the lines discussed by Ghahremani (1977).

References

Abeyaratne, R., Knowles, J.K., 1990. On the driving traction acting on a surface of strain discontinuity in a continuum. Journal of the Mechanics and Physics of Solids 38, 345–360.

Ball, J.M., James, R.D., 1987. Fine phase mixtures as minimizers of energy. Arch. Rat. Mech. Anal. 100, 13–52.

Ball, J.M., James, R.D., 1992. Proposed experimental tests of a theory of fine microstructure and the two well problem. Phil. Trans. R. Soc. London A338, 389–450.

Bruno, O.P., Reitich, F., Leo, P.H., 1996. The overall elastic energy of polycrystalline martensitic solids. J. Mech. Phys. Solids 44, 1051–1101.

Budiansky, B., Wu, T.T., 1962. Theoretical prediction of plastic strains of polycrystals. In: Proc. 4th U.S. National Congress of Applied Mechanics, 1175–1185.

Cao, H.C., Evans, A.G., 1993. Nonlinear deformation of ferroelectric ceramics. Journal of the American Ceramic Society 76, 890–896.

Chan, K.H., Hagood, N.W., 1994. Modelling of nonlinear piezoceramics for structural actuation. In: Hagood, N.W. (Ed.), Proceedings of SPIE, Smart Structural Materials, vol. 2190, p. 194.

Dunn, M.L., 1994. Electroelastic Green's functions for transversely isotropic piezoelectric media and their application to the solution of inclusion and inhomogeneity problems. International Journal of Engineering Science 32, 119–131.

Eshelby, J.D., 1957. The determination of the elastic field of an ellipsoidal inclusion, and related problems. Proc. Roy. Soc. Lond. A241, 376–396.

Gandhi, M.V., Thompson, B.S., 1992. Smart Materials and Structures. Chapman and Hall, London.

Ghahremani, F., 1977. Numerical evaluation of the stresses and strains in ellipsoidal inclusions in an anisotropic elastic material. Mech. Res. Comm. 4 (2), 89–91.

Hill, R., 1965a. A self-consistent mechanics of composite materials. J. Mech. Phys. Solids 13, 213–222.

Hill, R., 1965b. Continuum micro-mechanics of elastoplastic polycrystals. J. Mech. Phys. Solids 13, 89–101.

Hill, R., 1966. Generalized constitutive relations for incremental deformation of metal crystals by multislip. J. Mech. Phys. Solids 14, 95–102.

Hill, R., 1967. The essential structure of constitutive laws for metal composites and polycrystals. J. Mech. Phys. Solids 15, 79–95.

Huang, M., Brinson, L.C., 1998. A multivariant model for single crystal shape memory alloy behaviour. J. Mech. Phys. Solids 46, 1379–1409.

Huber, J.E., 1998. Ferroelectrics: models and applications. Ph.D. thesis, University of Cambridge.

Hutchinson, J.W., 1970. Elastic–plastic behaviour of polycrystalline metals and composites. Proc. Roy. Soc. Lond. A319, 247–272.

Hwang, S.C., Lynch, C.S., McMeeking, R.M., 1995. Ferroelectric/ferroelastic interactions and a polarization switching model. Acta Metallurgica et Materialia 43, 2073–2084.

Hwang, S.C., McMeeking R.M., 1998a. The prediction of switching in polycrystalline ferroelectric ceramics. Ferroelectrics 207, 465–495.

Hwang, S.C., McMeeking R.M., 1998b. A finite element model of ferroelectric polycrystals. Ferroelectrics 211, 177–194.

Hwang, S.C., McMeeking, R.M., 1998c. A finite element model of ferroelastic polycrystals. International Journal of Solids and Structures, to appear.

Hwang, S.C., Huber, J.E., McMeeking, R.M., Fleck, N.A., 1998. The simulation of switching in polycrystalline ferroelectric ceramics. Journal of Applied Physics 84, 1530–1540.

Jaffe, B., Cook, W.R., Jaffe, H., 1971. Piezoelectric Ceramics. Academic Press, London.

Jiang, Q., 1993. Macroscopic behavior of a bar undergoing the paraelectric–ferroelectric phase transformation. J. Mech. Phys. Solids 41, 1599–1635.

Jiang, Q., 1994. The driving traction acting on a surface discontinuity within a continuum in the presence of electromagnetic fields. Journal of Elasticity 34, 1.

Lagoudas, D.C., Bhattacharyya, A., 1997. On the correspondence between micromechanical models for isothermal pseudoelastic response of shape memory alloys and the Preisach model for hysteresis. Mathematics and Mechanics of Solids 2, 405–440.

Lines, M.E., Glass, A.M., 1977. Principles and Applications of Ferroelectrics and Related Materials. Oxford University Press.

Loge, R.E., Suo, Z., 1996. Nonequilibrium thermodynamics of ferroelectric domain evolution. Acta Materialia 44, 3429–3438.

Lynch, C.S., 1996. The effect of uniaxial stress on the electro-mechanical response of 8/65/35 PLZT. Acta Materialia 44, 4137.

Newnham, R.E., Xu, Q.C., Kumar, S., Cross, L.E., 1990. Smart Ceramics. Ferroelectrics 102, 77–89.

Nye, J.F., 1957.. Physical Properties of Crystals: Their Representation by Tensors and Matrices. Oxford University Press, p. 124.

Pepin, J.G., Boyland, W., 1989. Electrode-based causes of delamination in multilayer ceramic capacitors. Journal of the American Ceramic Society 72, 2287–2291.

Patoor, E., Eberhardt, A., Berveiller, M., 1994. Micromechanical modelling of shape memory behavior. In: Brinson, L.C., Moran, B. (Eds.), Mechanics of Phase Transformations and Shape Memory Alloys. ASME AMD 189, 23–37.

Smyshlyaev, V.P., Willis, J.R., 1998. A 'nonlocal' variational approach to the elastic energy minimisation of martensitic polycrystals. Proc. Roy. Soc. Lond. A454, 1573–1613.

Willis, J.R., 1965. The elastic interaction energy of dislocation loops in anisotropic media. Quart. J. Mech. Appl. Math. 18 (4), 419–433.

Winzer, S.R., Shankar, N., Ritter, A.P., 1990. Designing co-fired multilayer electrostrictive actuators for reliability. Journal of the American Ceramic Society 73, 2246–2257.